

Ultrafine Fully Vulcanized Natural Rubber Modified by Graft-Copolymerization with Styrene and Acrylonitrile Monomers

Krittaphorn Longsiri

Chulalongkorn University

Phattarin Mora

Srinakharinwirot University

Watcharapong Peeksumtiye

Chulalongkorn University

Chanchira Jubsilp

Srinakharinwirot University

Kasinee Hemvichian

Thailand Institute of Nuclear Technology

Panagiotis Karagiannidis

University of Sunderland

Sarawut Rimdusit (✉ sarawut.r@chula.ac.th)

Chulalongkorn University Faculty of Engineering

Research Article

Keywords: Graft copolymer, DPNR-g-(PS-co-PAN), UFPNR, Electron beam vulcanization, Spray drying

Posted Date: June 7th, 2022

DOI: <https://doi.org/10.21203/rs.3.rs-1640446/v1>

License: © ⓘ This work is licensed under a Creative Commons Attribution 4.0 International License.

[Read Full License](#)

Abstract

This research aims to modify ultrafine fully vulcanized powdered natural rubber (UFPNR) prepared by emulsion graft-copolymerization with styrene (St) and acrylonitrile (AN) monomers onto deproteinized natural rubber (DPNR). The effects of monomer content and St/AN weight ratio on grafting efficiency and thermal stability of the developed DPNR-g-(PS-co-PAN) were investigated. The results showed that grafting efficiency was enhanced up to 87% with weight ratio St:AN 80:20. The obtained DPNR-g-(PS-co-PAN) was radiated by an electron beam at various doses, followed by a spray drying process to produce UFPNR. The obtained modified UFPNR particles irradiated at dose up to 300 kGy were relatively spherical with a particle size of approximately 4.4 μm . Furthermore, the degradation temperature of 5wt% loss (T_{d5}) of UFPNR was found in the range of 349–356°C. The results revealed that the modified UFPNR is suitable as a toughening filler for a broader spectrum of polymers.

1. Introduction

Recently, ultrafine fully vulcanized powdered natural rubbers (UFPNRs) have become an alternative to traditional commodity synthetic rubber powder, due to renewable resources used for their preparation, which are environmentally friendly, reasonably priced. UFPNRs are illustrated to be suitable toughening fillers in a polymer matrix (Lin Y et al., 2021; Wongkumchai, Amornkitbamrung, Mora, Jubsilp, & Rimdusit, 2021). Ultrafine fully vulcanized powdered rubbers (UFPRs) were prepared by irradiation vulcanization followed by a spray drying process to produce a controllable spherical particle powder (Qiao J. et al., 2002). Mostly UFPRs were obtained from synthetic rubber latexes as raw materials, such as styrene-butadiene rubber (SBR) (X. Liu, Gao, Bian, & Wang, 2014), carboxylated-styrene butadiene rubber (XSBR) (Taewattana, Jubsilp, Suwanmala, & Rimdusit, 2018), acrylonitrile-butadiene rubber (NBR) (Pan & Liu, 2022; Wu, Xie, & Yang, 2010), and carboxylated-nitrile butadiene rubber (XNBR) (Huang et al., 2002; Taewattana et al., 2018). It is well known that UFPRs show predominantly reinforcement effect into other rubbers (Tian et al., 2006) or other polymer matrices and modify composite properties, such as reduction of the wear mass loss and friction coefficient of epoxy composite for friction materials (Yu, Hu, Ma, & Yin, 2008) increase the toughness or heat resistance of PVC (Q. Wang et al., 2005), epoxy resin (Huang et al., 2002), polypropylene (Y. Liu et al., 2004), and phenolic resin (Y. Liu, Fan, Ma, Tan, & Qiao, 2006; Ma et al., 2005). UFPRs possess good elasticity and are dispersed easily in polymer matrices during blending, as a result of their particular microstructure i.e. a spherical powder form with high crosslinking on the particle surface and moderate crosslinking in the inner part (Tian et al., 2006). Moreover, the advantages of UFPRs over the conventional rubber in a latex form are higher stability upon long-term storage and not harmful to the human body during blending (Qiao, 2020; J. Wang, Zhang, Jiang, & Qiao, 2019).

Despite the extensive use, unfortunately, the production of UFPNR is restricted, because of aggregation between particles (Taewattana et al., 2018). Therefore, NR has been developed by enhancing the degree of crosslinking by adding polyfunctional monomers as a crosslinking agent or coagent in the rubber latex before the irradiation process. Lin et al. (Lin Y et al., 2021) have studied the effect of acrylate coagents having different amounts of functional groups i.e. dipropylene glycol diacrylate (DPGDA), trimethylol

propane trimethacrylate (TMPTMA), and ditrimethylol propane tetraacrylate (DTMPTA), on properties of UFPNR produced by radiation vulcanization and spray-drying. They suggested that ditrimethylol propane tetraacrylate (DTMPTA), which had four functional acrylate groups, demonstrated high efficiency in enhancing the degree of crosslinking in NR that led to UFPNRs with much less agglomerated particles. However, NR which is a non-polar long chain hydrocarbon, lacks in some properties i.e. it has poor solvent resistance, and limited application due to its immiscibility when blended with polar polymers (W. Arayaprane, P. Prasassarakich, & G. L. Rempel, 2002; Kangwansupamonkon, Gilbert, & Kiatkamjornwong, 2005). Therefore, it is necessary to modify the properties of NR before processing to overcome these problems.

Chemical modification by graft copolymerization is one of the most attractive techniques. The NR molecular structure which contains cis-1,4-polyisoprene with an electron-donating methyl group attached to the carbon-carbon double bond in its main chain can facilitate the reaction with other vinyl monomers and covalently bonded onto the NR backbone. Several vinyl monomers have been used for grafting modification of NR, such as styrene (St) (T. Dung et al., 2016), acrylonitrile (AN) (Prukkaewkanjana, Kawahara, & Sakdapipanich, 2013), methyl methacrylate (MMA) (Kongparakul, Prasassarakich, & Rempel, 2008), and maleic anhydride (MA) (Pongsathit & Pattamaprom, 2018) to improve solvent resistance, thermal stability, mechanical properties, and compatibility of NR. Rimdusit et al. (Rimdusit et al., 2021) have improved thermal stability and solvent resistance of UFPNR via graft-copolymerization with polystyrene (PS) and polyacrylonitrile (PAN), respectively. The results revealed that the proper monomer content was 5 phr and proper radiation dose was 300 kGy for producing UFPNR-g-PS and UFPNR-g-PAN with maintaining rather high thermal stability. Therefore, the combination of St and AN monomer to form St/AN copolymer (SAN) by grafting on NR backbone is expected to improve the thermal stability the solvent resistance of NR and probably the compatibility with various polymer matrices having different polarity. (Angnanon, Prasassarakich, & Hinchiranan, 2011; T. A. Dung et al., 2017; Fukushima, Kawahara, & Tanaka, 1988; Indah Sari, Handaya Saputra, Bismo, & R. Maspanger, 2020; Nguyen Duy et al., 2020; Nguyen, Do, Tran, & Kawahara, 2019; Prasassarakich, Sintoorahat, & Wongwisetsirikul, 2001)

The present work is devoted on modifying UFPNR by graft-copolymerization with the combination of St and AN monomers onto deproteinized NR using tert-butyl hydroperoxide (TBHPO) and tetraethylenepentamine (TEPA) as a redox initiator. The effects of monomer contents and St/AN weight ratios of DPNR-g-(PS-co-PAN) on monomer conversion and grafting efficiency were determined. The obtained DPNR-g-(PS-co-PAN) were irradiated by an electron beam in the presence of DTMPTA as coagent followed by spray drying process to produce UFPNR. The effect of irradiation doses on the morphology and thermal properties of UFPNR was also investigated.

2. Experimental

2.1. Chemicals

High ammonia natural rubber (HANR) latex containing 60% of dry rubber content (DRC) was obtained from Sri Trang Agro-Industry Public Co., Ltd. (Thailand). Sodium dodecyl sulfate (SDS; 99%, Merck), urea (99.5%), magnesium-sulfate heptahydrate ($\text{MgSO}_4 \cdot 7\text{H}_2\text{O}$), styrene (99%), acrylonitrile (99%), tert-butyl hydroperoxide (TBHPO; 70% in water), tetraethylene pentamine (TEPA), di-trimethylolpropane tetraacrylate (DTMPTA), sodium hydroxide (NaOH), acetone (99.5%), and 2-butanone (99%) were purchased from Tokyo Chemical Industry Co., Ltd. (Tokyo, Japan).

2.2 Preparation of DPNR latex and purification of St and AN monomers

Deproteinized natural rubber (DPNR) was prepared by incubating HANR with 0.1 wt% urea and 1 wt% SDS at room temperature for 60 min, followed by centrifugation at 10,000 rpm, 15 °C for 30 min. After centrifugation, the cream fraction was redispersed in 0.5 wt% of SDS solution. The latex was washed repeated twice by centrifugation. The final product of DPNR latex was stabilized in 0.8 wt% of SDS solution and diluted to 30% DRC. (Kawahara, Klinklai, Kuroda, & Isono, 2004).

St and AN monomers were extracted with 10 wt% sodium hydroxide solution, washed with de-ionized water until neutral, and dried in MgSO_4 to remove inhibitor (T. A. Dung et al., 2017).

2.3 Graft copolymerization of DPNR with St and AN

The graft copolymerization of DPNR with St and AN in the latex state was conducted in 500 cm³ glass reactor equipped with a mechanical stirrer, water bath and nitrogen gas inlet. The DPNR latex and SDS were charged into a glass reactor under a nitrogen atmosphere and stirring at the speed of 400 rpm, 40 °C for approximately 2 hours. Afterwards, TEPA and TBHPO were used as an initiator at a concentration of 3.5×10^{-5} mol/g of dry rubber. St/AN monomers with a ratio 20/80, 30/70, 50/50, 70/30 or 80/20 wt% was added in a solution of dry rubber at concentration 1.5×10^{-3} mol/g (15 phr) or 0.5×10^{-3} mol/g of dry rubber (5 phr). Then, the grafting reaction was continued for 2.5 hours (Nguyen Duy et al., 2020).

After the reaction was finished, the unreacted monomers were removed by the rotary evaporator at 80 °C under reduced pressure for 1 hour. The mixture was cast in a glass Petri dish and dried to constant weight in a vacuum oven at 50 °C. The monomer conversion of graft copolymerization reaction was determined by the gravimetric method using the following equation: The increase in mass of grafted NR was equal to the amount of formed polymer and was used for the calculation of monomer conversion.

$$\text{Monomer conversion (\%)} = \frac{\text{weight of polymer in gross copolymer}}{\text{total weight of monomers}} \times 100$$

1

After drying, the product was extracted with a mixture of acetone/2-butanone in ratio 3/1 v/v for 48 hours by using a Soxhlet apparatus to remove the free homopolymer, i.e., PS, PAN, PS-co-PAN. The grafting efficiency was calculated as follows:

$$\text{Grafting efficiency (\%)} = \frac{\text{weight of polymer linked to NR}}{\text{total weight of the polymer formed}} \times 100$$

2

2.4 Preparation of Ultrafine Fully Vulcanized Powdered Rubber (UFPNR)

The grafted DPNR was diluted to 20% DRC with de-ionized water in the presence of 3 phr of DTMPTA. The latex mixture was stirred for 15 min before being vulcanized by electron beam irradiation at the doses of 100, 200, or 300 kGy supported by Thailand Institute of Nuclear Technology (Public Organization). Then, the vulcanized grafted DPNR was dried by a spray dryer (model B-290 from BUCHI, Switzerland) with the inlet temperature at 150°C, feed flow rate 7 ml/min, and air flow rate 500 L/hr. to achieve the ultrafine powdered rubbers as a bottom product.

2.5 Samples characterization

The chemical structure of DPNR-g-(PS-co-PAN) obtained after Soxhlet extraction was studied by using Fourier transform infrared spectroscopy (model 2000 FTIR, Perkin Elmer) with an attenuated total reflection (ATR) accessory (Waltham, Massachusetts, United States) in the range from 4000 to 600 cm^{-1} by averaging 128 scans at a resolution of 4 cm^{-1} . ^1H NMR spectra were recorded on Bruker AV500D spectrometer 500 MHz (Bruker, Switzerland) was also used to confirm the FTIR results. The samples were dissolved in deuterated chloroform (CDCl_3) using the pulse accumulation of 64 scans and LB parameter of 0.30Hz.

The morphology of NR latex particles was observed with a transmission electron microscope (TEM, model JEM-1400 from JEOL Ltd., Tokyo Japan) with an accelerating voltage of 80 kV. Before observation, one mL of NR latex (30% DRC) was diluted using 300 mL deionized water and placed on a carbon-coated copper grid. The NR latex was stained with 1.0 wt% osmium tetroxide (OsO_4) to enhance the resolution (Chueangchayaphan, Tanrattanakul, Chueangchayaphan, Muangsap, & Borapak; Gosecka & Gosecki, 2015; Schneider, Pith, & Lambra, 1996). After staining, the samples were dried in ambient air before observation.

After irradiation followed by spray drying process the obtained UFPNR was coated with thin gold using a JEOL ion sputtering device (model JFC-1200) for 4 min. The morphology was investigated by a scanning electron microscope (SEM, model JSM-6510A from JEOL Ltd., Tokyo Japan) with an accelerating voltage of 15 kV. The particle size of the UFPNR was measured by using the Image J program.

The change of polarity of NR after chemical modification was estimated by their wettability. The rubber films were prepared by drying latex under reduced pressure at room temperature for a week and examined by static contact angle (sessile drop) measurements using a contact angle meter (model DM300, Kyowa Interface Science Co., Ltd., Japan). Distilled water was used as the test liquid. The shape of the drops

was observed with a microscope equipped with a CCD camera, and the contact angles of the same sample were measured at least 5 times in ambient air, and an average value established.

The degradation temperature of the UFPNRs was evaluated by using a thermogravimetric analyzer (model TGA1 module from Mettler-Toledo, Thailand). The samples ~ 10 mg were heated from 25°C to 800°C with a heating rate of 20°C/min under nitrogen atmosphere at a nitrogen purge gas flow rate of 50 ml/min.

The glass transition temperature (T_g) of UFPNR was determined by using a differential scanning calorimeter (model DSC1 module from Mettler-Toledo, Thailand). The samples about ~ 10 mg were cooled to -100°C by liquid nitrogen and heated up to 25°C with a constant rate of 10°C/min under nitrogen atmosphere.

Swelling properties and gel content of UFRNR were then evaluated. The weight of UFPNR (W_1) was measured before immersing in toluene ($\rho_s = 0.87 \text{ g/cm}^3$, $V_1 = 106.5 \text{ ml/mol}$) at room temperature for 24 hours. After that, the swollen UFPNR was immediately weighted (W_2), followed by drying in a vacuum oven at 80°C for 24 hours to remove the solvent to obtain dried weight (W_3). The swelling ratio (Q), molecular weight between crosslinks (M_C), crosslink density (CLD) and gel fraction (g) were calculated by using the following equations (Flory-Rehner equation) (Flory & Rehner, 1943);

$$Q = \frac{(W_2 - W_1) / s}{W_1 / r}$$

3
.....

$$g = \frac{W_3}{W_1}$$

4
.....

$$M_C = \frac{-rV_1(\phi_r^{\frac{1}{3}} - \frac{\phi_r}{2})}{\text{Ln}(1 - \phi_r) + \phi_r + X_{12}\phi_r^2} : \text{where } \phi_r = \frac{1}{1 + Q}$$

5
.....

$$CLD = \frac{rN}{M_C} \dots\dots\dots(6)$$

Where W_1 , W_2 , and W_3 are the weights of initial, swollen and dried samples, respectively. ρ_s and ρ_r are the densities of solvent (0.87 g/cm³ of toluene) and rubber, φ_r is the volume fraction of polymer in the swollen sample, V_1 is the molar volume of the toluene solvent (106.5 ml/mol), χ_{12} is the polymer–solvent interaction parameter (the value of χ_{12} is 0.393 for toluene) and N is Avogadro's number (6.022×10^{23}).

3. Results And Discussion

3.1 Graft copolymerization of DPNR with St and AN

3.1.1 Effect of St/AN monomer ratio and monomer content on graft copolymerization

Monomers conversion of graft copolymerization reaction is the factor that evaluates the percentage of monomers converted to grafted copolymer and the amount of formed homopolymers. Grafted copolymer relates to the grafting efficiency, which is the amount of PS, PAN, and PS-co-PAN actually attached to the poly-isoprene chains by chemical linkage. Therefore, they cannot be eliminated by soxhlet extraction. At the same time, the monomers can be homopolymerised under the reaction conditions; the reaction occurs in the aqueous phase and the homopolymers are formed as short-chain free polymer products i.e., free-PS, eliminated by soxhlet extraction with a suitable solvent. The monomers conversion and grafting efficiency of DPNR-*g*-(PS-co-PAN) in the presence of St/AN at various weight ratio were estimated by gravimetric analysis using Eq. (1) and Eq. (2), respectively, as shown in Fig. 1 and Fig. 2. The monomer conversion at monomer content of 5 phr was found to be 23, 31, 38, 43, or 46%, whereas, the grafting efficiency was 26, 35, 37, 42, or 48% with an addition of St/AN weight ratio of 20/80, 30/70, 50/50, 70/30, or 80/20 respectively. It was found that monomers conversion and the grafting efficiency at monomer content of 5 phr was substantially increased with raising the amount of St. The most significant reason is that the solubility of the monomers in the aqueous and organic phase is responsible for the relative rate of monomer reaction. The St monomer being hydrophobic was similar to polarity of polyisoprene in NR. In contrast, AN monomer is a partially water-soluble monomer with relatively more affluent in the aqueous phase. For that reason, to increase the St monomer may preferentially react with polyisoprenyl macroradicals first to generate stable radical, which is styryl macroradicals (DPNR-*g*-St-) capable of further copolymerization with AN monomer (W. Arayapranee, P. Prasassarakich, & G. L. Rempel, 2002). Furthermore, St monomer can act as an electron donor to activate the carbon-carbon double bond of AN monomer, which is an electron acceptor by creating a charge transfer complex (CTC). In consequence, St-AN copolymers can be synthesized with the predominantly alternating structure to generate oligomer-radicals (AN-co-St-) which highly activates the weakly reactive double bond of AN towards the rubber macroradicals (Indah Sari, Handaya Saputra, Bismo, R. Maspanger, & Cifriadi, 2015; Ji, Liu, Huang, & Yan, 2005). The monomers conversion and the grafting efficiency at monomer content 15 phr showed the same trend but higher than those at the content 5 phr. The monomers conversion at monomer content 15 phr increased from 67, 74, 80, 86, to 89, as well as the grafting efficiency was increased from 69, 77, 79,

85, to 86% with St/AN weight ratio 20/80, 30/70, 50/50, 70/30, or 80/20, respectively. It can be explained that during the copolymerization at higher monomer content more monomer and oligomer radicals are produced which raised the chance of the reaction between monomer and oligomer radicals with NR molecules to form graft copolymer.

3.1.2 The Morphology of DPNR-g-(PS-co-PAN)

In the grafting process by emulsion copolymerization, the NR particles and droplets of undissolved monomers were stabilized by SDS surfactant molecules absorbed on their surfaces to form micelle particles. The mechanism of the emulsion copolymerization process takes place in the organic phase, which is inside the micelle particles, and very little occurs in the aqueous phase. To begin with, in our case the redox initiation system has two components that is, TBHPO which is a hydrophobic oxidizing agent and prefer to remain strongly into the organic phase or the NR surface, whereas the TEPA is a hydrophilic reducing agent prefers to remain in the aqueous phase. These were proposed to be thermally dissociated to generate initiator radicals ($I\cdot$) at the rubber/water interface to form grafting sites present on the surface of NR particles as shown in Fig. 3 (Schneider et al., 1996). In Fig. 4 are shown the initiator radicals possibly attached to active sites of the polyisoprene backbone in two ways. Through abstraction of an allylic hydrogen, which is the hydrogen in $-CH_2$ next to carbon-carbon double bond and transfer of the radical to form active site at allylic carbon and give secondary polyisoprene macroradicals (DPNR \cdot). Also, the initiator radicals might interact through an addition reaction at carbon-carbon double bond, breaking the double bond of rubber main chain to give tertiary polyisoprene macroradicals (DPNR \cdot) (Kochthongrasamee, Prasassarakich, & Kiatkamjornwong, 2006). At the same time, initiator radicals can attach to the St and AN monomers to form monomer and oligomer radicals i.e., (St \cdot), (AN \cdot), and (AN-co-St \cdot) (Staverman, 1979). In a second step, a propagating polymer chain can be formed in the presence of monomer radicals and macroradicals to form graft copolymer. The cycle of the growing chain of the polymer particle continues until the monomer conversion is essentially complete in the termination steps by chain transfer to macromolecules or combination reaction (Azanam & Ong, 2017).

As mentioned previously, the characteristic morphology of grafted DPNR (DPNR-g (PS-co-PAN)) particles was confirmed by TEM micrographs compared to virgin NR. The micrograph of virgin NR particles was shown in Fig. 5(a). The dark domains describe the electron-dens of the carbon-carbon double bonds of isoprene units inside the NR as spherical particles, with sharp edges and smooth surfaces (Chueangchayaphan et al., 2017; Gosecka & Gosecki, 2015). Meanwhile, the micrographs of grafted DPNR particles with monomer contents at 5 and 15 phr are shown in Fig. 5(b) and Fig. 5(c). The figures illustrated the contrast variation of electron density between the middle and the edge of particles. The dark domains at the middle were represented to DPNR particles attributing to the core-structure surrounding by the distinct brighter domains represented to the grafted PS-co-PAN phase attributing to the shell-structure (Schneider et al., 1996). The macroradical chains were generated onto the surface of DPNR particles while continuing to propagate to form the shell layer. Moreover, the thickness of the shell layer has $1.1 \pm 2.7 \mu\text{m}$ larger than that of virgin NR particles and forms a perfect shell at monomer content 15 phr ascribable to the highest grafting efficiency of grafted NR up to 86%. Since the active

grafting sites are totally occupied at maximum grafting, a sufficient percent of grafting was required to keep the bonding between core and shell strong enough to prevent the breaking of core-shell particles at the interphase.

The advantages of core-shell structure may prevent the agglomeration of the DPNR particles led to processing aids when produced UFPNR and improved interfacial adhesion between UFPNR and polymer matrix.

3.1.3 The Chemical Structures of DPNR-g-(PS-co-PAN)

The chemical structure of the grafted DPNR with St/AN monomer at weight ratio of 80/20 which showed the highest monomer conversion and grafting efficiency with different monomer content at 5 and 15 phr were investigated by FTIR spectroscopy. The chemical structure of the obtained grafted DPNR after soxhlet extraction was examined by comparing its FTIR signal with DPNR, and the results are plotted in Fig. 6. All FTIR spectra showed the characteristic absorption bands of NR. In the spectrum of DPNR shown in Fig. 6(a), the distinctive absorption peaks at 2915 and 2852 cm^{-1} corresponding to C-H stretching of $-\text{CH}_3$ and $-\text{CH}_2-$, respectively and the absorption band at 1664 cm^{-1} corresponding to vibration of C = C stretching are shown. C-H stretching vibration at $-\text{CH}_2-$ is expected around 1448 cm^{-1} and the absorption band at 1375 cm^{-1} is assigned to C-H asymmetry vibration of $-\text{CH}_3$. Additionally, the absorption band at 1244 cm^{-1} is attributed to vibration of C-C stretching next to C = C, which is ($\text{R}_2\text{C} = \text{CH}-\text{R}$) or at cis1,4 addition position, while the peak of 836 cm^{-1} indicated C = C bending vibration in NR main chain (Dinsmore & Smith, 1948; Kishore & Pandey, 1986; Nallasamy & Mohan, 2004). Confirmation of grafted NR by considering the spectrum of DPNA-g-(PS-co-PAN) with monomer content 5 phr is shown in Fig. 6(b). It could be pointed out by the existence of characteristic absorption bands at 1540–1600 cm^{-1} which is vibration of C = C stretching of styrenic benzene rings corresponding to absorbance bands at 760 and 700 cm^{-1} which relate to vibration of C-H bending of styrenic benzene rings of polystyrene (Nguyen Duy et al., 2020). Furthermore, the new absorption band appeared at wavenumber 2247 cm^{-1} ascribed to vibration of $\text{C} \equiv \text{N}$ stretching in PAN. In addition, the intensity of absorbance peak can imply the quantity of functional groups in graft copolymer. The spectrum of DPNA-g-(PS-co-PAN) with monomer content 15 phr is shown in Fig. 6(c). The intensity of absorption bands at 2247, 760, and 700 cm^{-1} obviously increased with increasing monomer content up to 15 phr., The intensity of the shoulder peak around 1650–1655 cm^{-1} and 833 cm^{-1} was decreased. This is due to the consumption of double bond (C = C) in NR structure during the grafting process.

The chemical structure of DPNA-g-(PS-co-PAN) with monomer content 5 and 15 phr were also analyzed by $^1\text{H-NMR}$ spectroscopy. The chemical shifts of NR at 1.61, 1.97 and 5.10 ppm, showed in Fig. 7 were attributed to the methyl proton CH_3 (c), unsaturated CH_2 (b, b') and olefinic proton (a), respectively (Pongsathit & Pattamaprom, 2018; Wongthong, Nakason, Pan, Rempel, & Kiatkamjornwong, 2013). Whereas the structure of St indicated the chemical shifts at 7.26 ppm attributed to the aromatic protons (d, d') were found (Pukkate et al., 2007), and the chemical shifts at 1.3–1.4 ppm (e), which corresponds to

the methylene protons (e) of DPNR linked to St in DPNR-g-(PS-co-PAN) was obtained (D. Liu, Kang, Chen, Liu, & Cao, 2013). Moreover, the chemical shifts appeared at 4.45 and 4.90 ppm assigned to the backbone protons (f, g) of AN units (Prukkaewkanjana et al., 2013). These results confirmed that grafting NR with St and AN can form DPNR-g-(PS-co-PAN) structure.

Previous research showed that only graft copolymerization of NR with St or AN was not sufficiently crosslinked the NR molecules to reduce aggregated and tackiness between rubber particles and could not be produced modified UFPNR. Therefore, the suggestion is that only suitable high crosslinking density of NR particles by irradiation could produce UFPNR and solve the aggregation problem (Rimdusit et al., 2021).

3.2 Characterizations of Ultrafine Fully Vulcanized NR Grafted with Polystyrene-co-Polyacrylonitrile (UFPNR-g-(PS-co-PAN))

The crosslinking process or vulcanization of NR molecules is obtained by electron beam vulcanization, which enhances crosslinking efficiency. Moreover, the crosslinking of NR can be further enhanced by adding polyfunctional monomers, known as a crosslinking coagent. Previous research (Lin Y et al.) suggested that the addition of 3 phr of DTMPTA could enhance crosslinking density and produce the smallest particle size of UFPNR. Therefore, DTMPTA at 3 phr was incorporated by electron beam irradiation in this research. The mechanism of DTMPTA irradiation by electron beam is shown in Fig. 8(a). The electrons released from electron beam accelerator would attack π -electrons at the double bonds on tetra functional groups of DTMPTA to form monomer free radicals.

Meanwhile, electron beam irradiation also attacks π -electrons at the double bonds on NR structure to form polymeric free radicals. After that, the highly active free radicals can react to form chemical linkage between DTMPTA and the NR structure. There are two possible ways to promote the formation of crosslinked networks. Firstly, the generated monomer free radicals would attach to the hydrogen at the AN segment on the grafted NR through hydrogen abstraction. Secondly, the generated monomer free radicals are attached with polymeric free radicals in NR chains to form crosslinked networks (Bee, Sin, Ratnam, Chew, & Rahmat, 2018). The possible structure of crosslinked UFPNR-g-(PS-co-PAN) in the presence of DTMPTA to form three-dimensional crosslinking network illustrated in Fig. 8(b).

3.2.1 The Chemical Structures of UFPNR-g-(PS-co-PAN)

The obtained UFPNR-g-(PS-co-PAN) at monomer content 15 phr with St/AN weight ratio 80/20, which provided the highest grafting efficiency was irradiated at different irradiation doses i.e. 100, 200, and 300 kGy. Their structure was studied by FTIR spectroscopy as illustrated in Fig. 9. The FTIR spectra showed the distinctive absorption peaks of NR at 836 cm^{-1} and $1650\text{--}1655\text{ cm}^{-1}$ corresponding to vibration of C = C bending and C = C stretching of NR main chain. Additionally, the absorption bands at 1080 and 1244 cm^{-1} is attributed to vibration of C-C stretching next to C = C, which is ($\text{R}_2\text{C} = \text{CH-R}$) or at cis1,4

addition position, while the peak of 836 cm^{-1} indicated C = C bending vibration in NR main chain. However, the intensity of the shoulder peak at $1650\text{--}1655\text{ cm}^{-1}$ corresponding to absorption peaks 1080 and 1244 cm^{-1} was decreased with increasing irradiation dose indicating the consumption of double bond (C = C) in NR structure to form C-C in three-dimensional crosslinking network. Additionally, the absorbance peak in range of $1755\text{--}1745\text{ cm}^{-1}$ exhibited the presence of ester group of DTMPA which promotes the crosslinking during irradiation vulcanization. Also, the additional high energy of irradiation decreased the intensity of absorption peak at 2242 cm^{-1} referred to nitrile group $\text{C}\equiv\text{N}$. Due to the sufficient energy the triple bond of $\text{C}\equiv\text{N}$ of AN was broken to form C=N bond (S. Badawy & A. Dessouki, 2003). From the results of chemical structure analysis, it can be concluded that NR grafted with St AN copolymer can be vulcanized to form three-dimensional crosslinking network by addition of DTMPA and concurrent electron beam irradiation.

3.2.2 The Effect of Electron Beam Irradiation on Gel Formation and Swelling Behaviors of UFPNR-g-(PS-co-PAN)

The swelling behavior of NR was evaluated in toluene to determine the ability to resist against this when immersed for 24 hours at room temperature. The parameters of swelling behaviour which determine the degree of crosslinking are the swelling ratio (Q), molecular weight between crosslinks (M_c), crosslinking density (CLD) and gel fraction (g) based on equations 4.3–4.6, respectively. The effect of used irradiation dose (100, 200, and 300 kGy) on these parameters for grafted NR at monomer content of 15 phr with St/AN 80/20 weight ratio are plotted in Fig. 10, and the numerical data were tabulated in Table 1. The results shown a significantly decreased swelling ratio from 17.52 ± 0.88 to 8.83 ± 0.54 when grafted NR was radiated with an electron beam 100 kGy. Moreover, the swelling ratio of the grafted NR decreased from 6.57 ± 0.44 to 4.99 ± 0.59 when the irradiation dose increased from 200 to 300 kGy, respectively. This can be explained by the sufficient electron beam irradiation which can activate the π -electrons of the double bonds and form highly active free radicals and a three-dimensional crosslinked network. Therefore, toluene molecules are more difficult to penetrate into the NR molecules. While the gel fraction continuously increased with the increase of irradiation dose. The results showed that the gel fraction increased from 0.58 ± 0.02 to 0.75 ± 0.02 and continues to increase from 0.89 ± 0.01 to 0.96 ± 0.01 when the irradiation dose increased from 200 to 300 kGy, respectively. This phenomenon was attributed to the long straight chain of NR, which has solubility parameter nearly that of toluene; while the molecules of the grafted NR chain have strong interaction with the toluene molecules which cause the expanding of NR chains and the swelling in the solvent eventually. Therefore, the increment of irradiation doses is extremely influential to gel fraction cause; it leads to increased inter-molecular crosslink between NR chains to form a three-dimensional crosslinking network that resists solvent penetration (Manshaie, Nouri Khorasani, Jahanbani Veshare, & Rezaei Abadchi, 2011; Tuti, Asep, Setijo, Dadi, & Adi, 2015).

Table 1 Swelling ratio, gel fraction, molecular weight between crosslinks and crosslink density of UFPNR-g-(PS-co-PAN)

UFPNR-g-(PS-co-PAN)	Swelling ratio (Q)	gel fraction (g)	M_c (g/mol)	CLD (mol/cm ³)
unirradiation	17.52 ± 0.88	0.58 ± 0.02	93,598 ± 8,388	0.83×10 ⁻²² ± 0.09
100 kGy	8.83 ± 0.54	0.75 ± 0.02	27,336 ± 7,022	1.54×10 ⁻²² ± 0.09
200 kGy	6.57 ± 0.44	0.89 ± 0.01	14,161 ± 4,610	2.13×10 ⁻²² ± 0.07
300 kGy	4.99 ± 0.59	0.96 ± 0.01	10,434 ± 2,932	2.45×10 ⁻²² ± 0.05

3.2.3 The Effect of Electron Beam Irradiation on Molecular Weight between crosslinks and Crosslink Density of UFPNR-g-(PS-co-PAN)

The effect of irradiation dose on the crosslink density, and molecular weight between crosslinks of grafted NR at monomer content 15 phr with St/AN 80/20 weight ratio after irradiation at 100, 200, and 300 kGy, are plotted in Fig. 11. The crosslink density of unirradiated grafted NR was $0.83 \times 10^{-22} \pm 0.09$ whereas crosslink density values of radiated grafted NR increased from $1.54 \times 10^{-22} \pm 0.09$, $2.13 \times 10^{-22} \pm 0.07$ and $2.45 \times 10^{-22} \pm 0.05$ with increasing irradiation dose from 100, 200, or 300 kGy respectively. Due to the influence of higher energy irradiation doses, the thermal energy stimulated rubber latex to promote more free radicals, which are more suitable to form a three-dimensional crosslinking network. This behavior causes hindrance of solvent penetration into NR molecules leading to reduce the swelling ratio. While, as expected, the molecular weight between crosslinks decreased with increasing the irradiation dose.

3.2.4 The Effects of Irradiation Doses on Morphology of UFPNR-g-(PS-co-PAN)

The grafted NR with St/AN weight ratio 80/20 having the highest grafting efficiency at monomer contents of 5 and 15 phr was prepared by irradiation with electron beam of 100, 200, or 300 kGy, followed by spray drying process to produce modified UFPNRs. The morphology of modified UFPNRs was observed by SEM. SEM micrographs of the modified UFPNR with monomer content of 5 phr with irradiation dose at 100 kGy are shown in Fig. 12(a). The modified UFPNR still shows aggregated and tacky rough surfaces and uncertain spherical particles, because of the amount of electron beam, which was not sufficient enough to generate free radicals for crosslinking. When increasing the irradiation dose to 200 and 300 kGy as shown in Fig. 12(b) and Fig. 12(c), respectively, the aggregation of modified UFPNR tended to be less at higher irradiation doses, and the particles showed the least aggregation at irradiation dose of 300 kGy.

Figure 13(a) shows SEM micrographs of the modified UFPNR with monomer content 15 phr at irradiation dose 100 kGy. Particles of UFPNR with more smooth surface are observed when compared to modified UFPNR with monomer content of 5 phr with irradiation dose of 100 kGy (Fig. 12.a). However, particles still showed aggregation, high tackiness and are uncertain spherical. When increasing the irradiation dose at

200 and 300 kGy as shown in Fig. 13(b) and Fig. 13(c), respectively, the aggregation of modified UFPNR tended to be less at higher irradiation doses and the particles showed the least aggregation at irradiation dose of 300 kGy. This results show the influence of irradiation dose on free radicals generation which form a three-dimensional crosslinking network, and reduce tackiness of rubber lattices leading to low aggregation and smooth surface particles, along with the smaller particle sizes (Rezaei Abadchi & Jalali-Arani, 2014). In addition, it was observed that an increase of doses resulted in a systematically decrease in the resulting rubber particle size. This phenomenon is attributed to the simultaneous mainchain scission and crosslinking of the rubber macromolecules occur during irradiation process particularly at higher dose of electron beam. From SEM micrographs, and the swelling behaviour study, it can be concluded that the increment of electron beam irradiation at 300 kGy is suitable for production of modified UFPNR.

3.2.5 The Effect of Grafting Efficiency on Morphology of UFPNR-g-(PS-co-PAN)

The virgin NR and the grafted NR with St/AN weight ratio 80/20 having the highest grafting efficiency at monomer contents at 5 and 15 phr was prepared by irradiation with electron beam with 300 kGy absorption dose, followed by spray drying process to produced UFPNR and modified UFPNRs. Figure 14 shows their SEM micrographs; aggregation of rubber particles was observed in virgin UFPNR which tended to fuse with each other although at increment irradiation dose up to 300 kGy. Different morphology in modified UFPNR at monomer content 5 and 15 phr is observed in Fig. 14(b) and Fig. 14(c), respectively. It can be seen that the morphology of modified UFPNR show non-aggregated and relatively spherical particles with relatively smooth surface and similar uniform particle size distribution.

The average particle sizes of the modified UFPNRs were measured from 500 particles, the results obtained are shown in Fig. 15, and the numerical data are tabulated in Table 2. It was found that the average particle sizes of the modified UFPNR were 3.56 ± 1.70 and 4.38 ± 1.79 μm at monomer content 5 and 15 phr, respectively; due to higher grafting efficiency at monomer content, 86% for 15 phr than 48% for 5 phr. This may be the reason that the particles are slightly larger.

Table 2
Particle sizes of the modified UFPNR

Monomer contents (phr)	St/AN monomer (wt%)	Grafting efficiency (%)	Irradiation doses (kGy)	Average particle size (μm)
5	80/20	48	300	3.56 ± 1.70
15	80/20	86	300	4.38 ± 1.79

3.2.6 The Effects of Monomer Ratio on Surface Properties of UFPNR-g-(PS-co-PAN)

The measurement of water contact angle is one of the conventional methods for estimating the hydrophilicity of polymer surfaces. PS-co-PAN was purposely grafted to the NR molecule to improve its affinity with the polar surfaces of NR, which was used to produce UFPNR. Profiles of water contact angle on the surfaces of unmodified NR and grafted NR are illustrated in Fig. 16. The contact angle of NR showed the highest value $71 \pm 0.1^\circ$ indicating the lowest hydrophilicity (Cabrera et al., 2017). While compared to grafted NR, the contact angle of the films was reduced from $56 \pm 0.1^\circ$ to $40 \pm 0.3^\circ$ and the lowest contact angle appeared at $27 \pm 0.7^\circ$ by increasing the AN content from 20, 50, and 80 wt%, respectively. The decrease in the water contact angle of NR after grafting modification is attributed to the presence of grafted poly(St-co-AN) chains on to NR surfaces as mentioned before at TEM analysis. As the AN groups present in the grafted poly(St-co-AN) are capable of hydrogen bonding with water molecules, they facilitate the spreading and wetting of a water drop on an NR surface. This would lead to a noticeable reduction in the water contact angle as the AN content increases, enhancing the hygroscopic characteristic of NR (Safeeda Nv, Gopinathan, Indumathi, Thomas, & Bhattacharyya, 2016).

3.2.7 The Effect of Grafting Efficiency on Thermal Stability of UFPNR-g-(PS-co-PAN)

The effect of grafting efficiency and irradiation dose on thermal stability, i.e., the degradation temperature at 5% weight loss (T_{d5}) which is a vital property indicating their performance at elevated temperatures was studied. In Fig. 17 TGA thermograms of virgin UFPNR and the modified UFPNR are shown, and the numerical data are presented in Table 3. It was found that T_{d5} of the virgin NR without irradiation was 334°C and increased to 344°C after irradiation with 300 kGy. This is because the electron beam provides radical reactions by activating the double bond of NR structure and tetra-acrylate groups of DTMPA to generate highly reactive radicals to form intermolecular and intramolecular C-C bonds in NR chains or three-dimension network structure (Akiba & Hashim, 1997; Dawes, Glover, & Vroom, 2007). Whereas C-C single bond is more stable than C = C double bonds, the crosslinks of NR chains can stabilize and restrict molecular mobility; more thermal energy is required to cause destructive changes leading to enhancement of T_{d5} (Bandzierz, 2018).

Then, the modified UFPNRs' degradation temperature was evaluated by considering, T_{d5} of unmodified UFPNR and modified UFPNR under the same irradiation dose at 300 kGy. It was found that T_{d5} was increased from 344 of unmodified UFPNR to 350 and 356°C for UFPNR-g-(PS-co-PAN) with monomer content 5 and 15 phr, respectively. As a result grafting with St-AN copolymer onto NR molecules improves T_{d5} of UFPNR. Besides the interaction of polar molecules between AN and NR. Moreover, the free radicals generated during the irradiation process would abstract the hydrogen attached to the AN section in rubber structure to form crosslinked networks of PAN (S. M. Badawy & A. M. Dessouki, 2003; Park, Choi, Lee, Kim, & Park, 2014; Xue, McKinney, & Wilkie, 1997).

Furthermore, at high grafting efficiency at monomer contents, 15 phr (i.e. 78%) were higher than that of 5 (i.e. 37%). The presence of St in the rubber increased, leading to the bulky side chains of aromatic rings grafted on the NR backbone resulted in greater difficulty for the polymers to flow or to slide past each other and generally led to a simultaneous increase in the chain stiffness of the modified UFPNRs. Therefore, the thermal stability was enhanced by grafting with PS-co-PAN (Seleem, Hopkins, Olivio, & Schiraldi, 2017).

The results can conclude that the modified UFPNRs by grafting with styrene-co-acrylonitrile at monomer content 15 phr can be improved T_{d5} 12 °C when compared to unmodified UFPNR, and improved T_{d5} 22 °C when compared to virgin NR.

Table 3
The degradation temperature at 5% weight loss (T_{d5}) at various monomer content

Sample	Monomer contents (phr)	ST/AN (wt%)	Irradiation doses (kGy)	T_{d5} (°C)
Unmodified NR	-	-	Unradiated	334
Unmodified UFPNR	-	-	300	344
UFPNR-g-(PS-co-PAN)	5	50/50	300	350
UFPNR-g-(PS-co-PAN)	15	50/50	300	356

3.2.8 The Effects of Monomer Ratio on Thermal Stability of UFPNR-g-(PS-co-PAN)

The effect of the St/AN weight ratio of UFPNR-g-(PS-co-PAN) with monomer content 15 phr at irradiation dose 300 kGy on the 5% weight loss (T_{d5}) was studied. TGA thermograms shown as Fig. 18 and the numerical data were tabulated in Table 4. The results found that an increase in T_{d5} of the UFPNR-g-(PS-co-PAN) with raising the styrene in St/AN weight ratio of 20/80, 30/70 and 50/50 cause incline in T_{d5} from 351 to 354 and highest at 356 °C, respectively, due to the increase of monomer conversion and grafting efficiency. Including the sufficient irradiation dose at 300 kGy can activate the double bond of NR structure and coagent to generate highly reactive radicals to form a three-dimensional network. This leads to higher heat energy consumption to destructive the polymer chains. However, raising the amount of St in St/AN weight ratio up to 70/30 and 80/20 resulted in T_{d5} of the UFPNR-g-(PS-co-PAN) decline to 352 and 349 °C, respectively. The results can be implied that as the percentage of St is increased (≥ 70 wt%) the aromatic benzene rings of the St units provide high irradiation resistance by high stability

resonance structure (Hassan, 2008; Witt, 1959). The physical properties of PS remain relatively stable even after high doses of irradiation, this phenomenon can generate low reactivity free radicals by the resonance in aromatic rings through to the backbone chains generate low reactivity free radicals, which determine chain scission could be induced in a NR molecule to counterbalance the effects of crosslinking (Bee et al., 2018; Burlant, Neerman, & Serment, 1962). Moreover, the benzene rings also cause high stiffness and low flexibility of NR chain resulting in block radical neighbour chains or partner macroradical to form crosslink network leading to chain scission of rubber chain (Bandzierz, 2018). Therefore, thermal stability can imply this phenomenon predominantly undergo chain scission in the NR backbone leads to give the shorter chains and reduce the degree of crosslinked networks when subjected to high energy radiation.

Table 4
The degradation temperature at 5% weight loss (T_{d5}) at various monomer content

Sample	Monomer contents (phr)	ST/AN (wt%)	Irradiation doses (kGy)	T_{d5} (°C)
Unmodified NR	-	-	300	334
UFPNR-g-(PS-co-PAN)	15	20/80	300	351
UFPNR-g-(PS-co-PAN)	15	30/70	300	354
UFPNR-g-(PS-co-PAN)	15	50/50	300	356
UFPNR-g-(PS-co-PAN)	15	70/30	300	352
UFPNR-g-(PS-co-PAN)	15	80/20	300	349

3.2.9 The Glass transition temperature of UFPNR-g-(PS-co-PAN)

T_g was determined by a DSC as shown in Fig. 19 and the numerical data were tabulated in Table 5. The results found that the T_g of virgin NR is -64 °C and increased to -63 °C when irradiated with electron beam 300 kGy. Because of increasing of irradiation dose due to the high three-dimensional network structure in radiated UFPNR-g-(PS-co-PAN) is attributed to the restriction imposed on the chain movement due to the crosslinking, as there are lesser number of free chains available at glassy to rubbery transition (Rezaei Abadchi & Jalali-Arani, 2014; Taewattana et al., 2018). Therefore, modified UFPNR with monomer content of 5 and 15 phr at 50/50 of St/AN weight ratio radiated at doses of 300 kGy are representative to

investigate the T_g which are -62 °C. It is possible that the bulky styrenic benzene ring of PS side chains can interact with neighbouring chains and restrict their rotational freedom. Also, intermolecular forces in grafted copolymers increased due to the introduction of polar nitrile groups in PAN at interface of NR and may cause movement limitation of NR chain. However, It can be seen that the effects of irradiation doses on T_g of modified UFPNRs were slightly increased compared with un-irradiated NR, which is about -64 °C, agreeing with previous work (Lin Y et al., 2021; Taewattana et al., 2018; Wongkumchai et al., 2021).

Table 5
Glass transition temperature (T_g) of UFPNR

Sample	Monomer contents (phr)	ST/AN ratio (wt%)	Irradiation dose (kGy)	T_g (°C)
Unmodified NR	-	-	-	-64
Unmodified UFPNR	-	-	300	-63
UFPNR-g-(PS-co-PAN)	5	50/50	300	-62
UFPNR-g-(PS-co-PAN)	15	50/50	300	-62

Conclusions

The modified NR latex, DPNR-g-(PS-co-PAN), was successfully prepared by grafting St-AN co-monomers onto DPNR latex via emulsion copolymerization confirmed by FTIR spectra and ^1H NMR spectra. The addition of St monomer up to St/AN weight ratio of 80/20 at monomer content of 15 phr provided the highest monomer conversion and grafting efficiency at 89 and 87%, respectively. Moreover, the DPNR-g-(PS-co-PAN) having desirable core-shell morphology is confirmed by TEM micrographs. The obtained modified NR has qualified to produce modified UFPNR by radiated with an electron beam in the presence of DTMPTA as a coagent followed by the spray drying process to produce UFPNR. The results revealed that the irradiation dose 300 kGy resulted in improved solvent resistance of the UFPNR-g-(PS-co-PAN) by reducing swelling ratio and molecular weight between crosslinks. The grafting and irradiation can improve the morphology of UFPNR particles, which are relatively spherical and show a non-aggregated smooth surface with a particle size of approximately 4.4 ± 1.8 μm . Thermal stability i.e. degradation temperature at 5% weight (T_{d5}) of the UFPNR modified by grafted with various St/AN weight ratios at monomer content, 15 phr was found to be in a range of 349 to 356°C. On the contrary, the T_g of modified UFPNR and unmodified UFPNR were not significantly enhanced and consequently they maintain the elastomeric properties of the UFPNR. Furthermore, the contact angle measurement result revealed that the modified UFPNR is suitable for utilizing as toughening filler for wide polarity and types of polymers.

Declarations

Ethics approval and consent to participate

Not applicable.

Consent for publication

Not applicable.

Availability of data and materials

All data analyzed during this study are included in this article.

Competing interests

The authors declare that they have no competing interests.

Funding

The authors would like to express their sincere appreciations to The National Research Council of Thailand (NRCT) and Fundamental Fund (FF) under Thailand Science Research and Innovation (TSRI) for financial support throughout the research. This research was also funded by the 90TH Anniversary of Chulalongkorn University Scholarship (50 3/2564), Chulalongkorn University and Thailand Institute of Nuclear Technology (public organization), Thailand, through its program of TINT to University.

Authors' contributions

Conceptualization and design of the research, K.L. and P.M.; experimental work, K.L. and W.P.; design of the research and discussion of the results, K.H., C.J. and K.L.; writing—original draft of the manuscript, K.L. and P.M.; writing—review and editing, P.K. and S.R.; supervision, conceptualization, and funding acquisition, S.R. All authors have read and agreed to the published version of the manuscript.

Acknowledgements

Electron beam irradiation was supported by Thailand Institute of Nuclear Technology (Public Organization).

References

1. Akiba, M., & Hashim, A. S. (1997). Vulcanization and crosslinking in elastomers. *Progress in Polymer Science*, 22(3), 475-521. doi:[https://doi.org/10.1016/S0079-6700\(96\)00015-9](https://doi.org/10.1016/S0079-6700(96)00015-9)
2. Angnanon, S., Prasassarakich, P., & Hinchiranan, N. (2011). Styrene/Acrylonitrile Graft Natural Rubber as Compatibilizer in Rubber Blends. *Polymer-Plastics Technology and Engineering*, 50(11), 1170-1178. doi:10.1080/03602559.2011.574667

3. Arayaprane, W., Prasassarakich, P., & Rempel, G. L. (2002). Synthesis of graft copolymers from natural rubber using cumene hydroperoxide redox initiator. *Journal of Applied Polymer Science*, *83*, 2993-3001. doi:10.1002/app.2328
4. Arayaprane, W., Prasassarakich, P., & Rempel, G. L. (2002). Synthesis of graft copolymers from natural rubber using cumene hydroperoxide redox initiator. *Journal of Applied Polymer Science*, *83*(14), 2993-3001. doi:https://doi.org/10.1002/app.2328
5. Azanam, S. H., & Ong, S. K. (2017). Natural Rubber and its Derivatives. In *Elastomers*.
6. Badawy, S., & Dessouki, A. (2003). Cross-Linked Polyacrylonitrile Prepared by Radiation-Induced Polymerization Technique. *The Journal of Physical Chemistry B*, *107*, 11273-11279. doi:10.1021/jp034603j
7. Badawy, S. M., & Dessouki, A. M. (2003). Cross-Linked Polyacrylonitrile Prepared by Radiation-Induced Polymerization Technique. *The Journal of Physical Chemistry B*, *107*(41), 11273-11279. doi:10.1021/jp034603j
8. Bandzierz, K. S., Reuvekamp, Louis A. E. M., Przybytniak, Grażyna, D., Wilma K., Blume, A., and Bieliński, D.M. (2018). Effect of electron beam irradiation on structure and properties of styrene-butadiene rubber. *Radiation Physics and Chemistry*, *149*, 14-25. doi:https://doi.org/10.1016/j.radphyschem.2017.12.011
9. Bee, S.-T., Sin, L. T., Ratnam, C. T., Chew, W. S., & Rahmat, A. R. (2018). Enhancement effect of trimethylpropane trimethacrylate on electron beam irradiated acrylonitrile butadiene styrene (ABS). *Polymer Bulletin*, *75*(11), 5015-5037. doi:10.1007/s00289-018-2316-z
10. Burlant, W., Neerman, J., & Serment, V. (1962). γ -radiation of p-substituted polystyrenes. *Journal of Polymer Science*, *58*(166), 491-500. doi:https://doi.org/10.1002/pol.1962.1205816627
11. Cabrera, F. C., Dognani, G., Santos, R. J., Agostini, D. L. S., Cruz, N. C., & Job, A. E. (2017). Surface Modification of Natural Rubber by Sulfur hexafluoride (SF₆) Plasma Treatment: A New Approach to Improve Mechanical and Hydrophobic Properties. *Journal of Coating Science and Technology*, *3*(3), 116-120. doi:10.6000/2369-3355.2016.03.03.3
12. Chueangchayaphan, W., Tanrattanakul, V., Chueangchayaphan, N., Muangsap, S., & Borapak, W. (2017). Synthesis and thermal properties of natural rubber grafted with poly(2-hydroxyethyl acrylate). *Journal of Polymer Research*, *24*(7). doi:10.1007/s10965-017-1269-5
13. Dawes, K., Glover, L. C., & Vroom, D. A. (2007). The Effects of Electron Beam and γ -Irradiation on Polymeric Materials. In (pp. 867-887).
14. Dinsmore, H. L., & Smith, D. C. (1948). Analysis of Natural and Synthetic Rubber by Infrared Spectroscopy. *Analytical Chemistry*, *20*(1), 11-24. doi:10.1021/ac60013a004
15. Dung, T., Nhan, N., Thuong, N., Nghia, P., Yamamoto, Y., Kosugi, K., . . . Thuy, T. (2016). Modification of Vietnam Natural Rubber via Graft Copolymerization with Styrene. *Journal of the Brazilian Chemical Society*. doi:10.21577/0103-5053.20160217
16. Dung, T. A., Nhan, N. T., Thuong, N. T., Viet, D. Q., Tung, N. H., Nghia, P. T., . . . Thuy, T. T. (2017). Dynamic Mechanical Properties of Vietnam Modified Natural Rubber via Grafting with Styrene.

17. Flory, P. J., & Rehner, J. (1943). Statistical Mechanics of Cross-Linked Polymer Networks I. Rubberlike Elasticity. *The Journal of Chemical Physics*, 11(11), 512-520. doi:10.1063/1.1723791
18. Fukushima, Y., Kawahara, S., & Tanaka, Y. (1988). Synthesis of graft copolymers from highly deproteinised natural rubber. *Journal of Rubber Research*, 1, 154-166.
19. Gosecka, M., & Gosecki, M. (2015). Characterization methods of polymer core–shell particles. *Colloid and Polymer Science*, 293(10), 2719-2740. doi:10.1007/s00396-015-3728-z
20. Hassan, M. M. (2008). Mechanical, thermal, and morphological behavior of the polyamide 6/acrylonitrile–butadiene–styrene blends irradiated with gamma rays. *Polymer Engineering & Science*, 48(2), 373-380. doi:10.1002/pen.20959
21. Huang, F., Liu, Y., Zhang, X., Wei, G., Gao, J., Song, Z., . . . Qiao, J. (2002). Effect of Elastomeric Nanoparticles on Toughness and Heat Resistance of Epoxy Resins. *Macromolecular Rapid Communications*, 23, 786-790. doi:10.1002/1521-3927(20020901)23:13<786::AID-MARC786>3.0.CO;2-T
22. Indah Sari, T., Handaya Saputra, A., Bismo, S., & R. Maspanger, D. (2020). Deproteinized Natural Rubber Grafted with Polyacrylonitrile (PAN)/Polystyrene (PS) and Degradation of its Mechanical Properties by Dimethyl Ether. *International Journal of Technology*, 11(1). doi:10.14716/ijtech.v11i1.1942
23. Indah Sari, T., Handaya Saputra, A., Bismo, S., R. Maspanger, D., & Cifriadi, A. (2015). The Effect of Styrene Monomer in the Graft Copolymerization of Acrylonitrile onto Deproteinized Natural Rubber. *International Journal of Technology*, 6(7). doi:10.14716/ijtech.v6i7.1266
24. Ji, B., Liu, C., Huang, W., & Yan, D. (2005). Novel Hyperbranched predominantly Alternating Copolymers Made From A Charge Transfer Complex monomer pair of p-(chloromethyl)styrene and Acrylonitrile via Controlled Living Radical Copolymerization. *Polymer Bulletin*, 55(3), 181-189. doi:10.1007/s00289-005-0429-7
25. Kangwansupamonkon, W., Gilbert, R. G., & Kiatkamjornwong, S. (2005). Modification of Natural Rubber by Grafting with Hydrophilic Vinyl Monomers. *Macromolecular Chemistry and Physics*, 206(24), 2450-2460. doi:https://doi.org/10.1002/macp.200500255
26. Kawahara, S., Klinklai, W., Kuroda, H., & Isono, Y. (2004). Removal of proteins from natural rubber with urea. *Polymers for Advanced Technologies*, 15(4), 181-184. doi:10.1002/pat.465
27. Kishore, K., & Pandey, H. K. (1986). Spectral studies on plant rubbers. *Progress in Polymer Science*, 12(1), 155-178. doi:http://dx.doi.org/10.1016/0079-6700(86)90008-0
28. Kochthongrasamee, T., Prasassarakich, P., & Kiatkamjornwong, S. (2006). Effects of redox initiator on graft copolymerization of methyl methacrylate onto natural rubber. *Journal of Applied Polymer Science*, 101(4), 2587-2601. doi:10.1002/app.23997
29. Kongparakul, S., Prasassarakich, P., & Rempel, G. L. (2008). Effect of grafted methyl methacrylate on the catalytic hydrogenation of natural rubber. *European Polymer Journal*, 44(6), 1915-1920. doi:10.1016/j.eurpolymj.2007.09.021

30. Lin Y, Amornkitbamrung L, Mora P, J. C., Hemvichian K, Soottitantawat A, Ekgasit S, & S., R. (2021). Effects of Coagent Functionalities on Properties of Ultrafine Fully Vulcanized Powdered Natural Rubber Prepared as Toughening Filler in Rigid PVC. *Polymers*, *13*(2), 289. doi:10.3390/polym13020289
31. Liu, D., Kang, J., Chen, P., Liu, X., & Cao, Y. (2013). ¹H NMR and ¹³C NMR Investigation of Microstructures of Carboxyl-Terminated Butadiene Acrylonitrile Rubbers. *Journal of Macromolecular Science, Part B*, *52*(1), 127-137. doi:10.1080/00222348.2012.695622
32. Liu, X., Gao, Y., Bian, L., & Wang, Z. (2014). Preparation and characterization of natural rubber/ultrafine full-vulcanized powdered styrene–butadiene rubber blends. *Polymer Bulletin*, *71*(8), 2023-2037. doi:10.1007/s00289-014-1169-3
33. Liu, Y., Fan, Z., Ma, H., Tan, Y., & Qiao, J. (2006). Application of nano powdered rubber in friction materials. *Wear*, *261*(2), 225-229. doi:http://dx.doi.org/10.1016/j.wear.2005.10.011
34. Liu, Y., Zhang, X., Gao, J., Huang, F., Tan, B., Wei, G., & Qiao, J. (2004). Toughening of polypropylene by combined rubber system of ultrafine full-vulcanized powdered rubber and SBS. *Polymer*, *45*(1), 275-286. doi:10.1016/j.polymer.2003.11.001
35. Ma, H., Wei, G., Liu, Y., Zhang, X., Gao, J., Huang, F., . . . Qiao, J. (2005). Effect of elastomeric nanoparticles on properties of phenolic resin. *Polymer*, *46*(23), 10568-10573. doi:10.1016/j.polymer.2005.07.103
36. Manshaie, R., Nouri Khorasani, S., Jahanbani Veshare, S., & Rezaei Abadchi, M. (2011). Effect of electron beam irradiation on the properties of natural rubber (NR)/styrene–butadiene rubber (SBR) blend. *Radiation Physics and Chemistry*, *80*(1), 100-106. doi:10.1016/j.radphyschem.2010.08.015
37. Nallasamy, P., & Mohan, S. (2004). Vibrational spectra of cis-1,4-polyisoprene. *Arabian Journal for Science and Engineering*, *28*(1 A), 17-26. Retrieved from <https://www.scopus.com/inward/record.uri?eid=2-s2.0-2942662209&partnerID=40&md5=402b9d6680d74fa05bcfb7c5c3377b58>
38. Nguyen Duy, H., Rimdusit, N., Tran Quang, T., Phan Minh, Q., Vu Trung, N., Nguyen, T. N., . . . Tran Thi, T. (2020). Improvement of thermal properties of Vietnam deproteinized natural rubber via graft copolymerization with styrene/acrylonitrile and diimide transfer hydrogenation. *Polymers for Advanced Technologies*, *32*(2), 736-747. doi:10.1002/pat.5126
39. Nguyen, T. H., Do, Q. V., Tran, A. D., & Kawahara, S. (2019). Preparation of hydrogenated natural rubber with nanomatrix structure. *Polymers for Advanced Technologies*, *31*(1), 86-93. doi:10.1002/pat.4749
40. Pan, C., & Liu, P. (2022). Fluorinated nitrile-butadiene rubber (F-NBR) via metathesis degradation: Closed system or open system? *European Polymer Journal*, *162*, 110886. doi:<https://doi.org/10.1016/j.eurpolymj.2021.110886>
41. Park, M., Choi, Y., Lee, S.-Y., Kim, H.-Y., & Park, S.-J. (2014). Influence of electron-beam irradiation on thermal stabilization process of polyacrylonitrile fibers. *Journal of Industrial and Engineering Chemistry*, *20*(4), 1875-1878. doi:10.1016/j.jiec.2013.09.006

42. Pongsathit, S., & Pattamaprom, C. (2018). Irradiation grafting of natural rubber latex with maleic anhydride and its compatibilization of poly(lactic acid)/natural rubber blends. *Radiation Physics and Chemistry*, 144, 13-20. doi:10.1016/j.radphyschem.2017.11.006
43. Prasassarakich, P., Sintoorahat, P., & Wongwisetsirikul, N. (2001). Enhanced Graft Copolymerization of Styrene and Acrylonitrile onto Natural Rubber. *JOURNAL OF CHEMICAL ENGINEERING OF JAPAN*, 34(2), 249-253. doi:10.1252/jcej.34.249
44. Prukkaewkanjana, K., Kawahara, S., & Sakdapipanich, J. (2013). Influence of Reaction Conditions on the Properties of Nano-matrix Structure Formed by Graft-Copolymerization of Acrylonitrile onto Natural Rubber. *Advanced Materials Research*, 844, 365-368. doi:10.4028/www.scientific.net/AMR.844.365
45. Pukkate, N., Kitai, T., Yamamoto, Y., Kawazura, T., Sakdapipanich, J., & Kawahara, S. (2007). Nano-matrix structure formed by graft-copolymerization of styrene onto natural rubber. *European Polymer Journal*, 43(8), 3208-3214. doi:10.1016/j.eurpolymj.2007.04.037
46. Qiao, J. (2020). Elastomeric nano-particle and its applications in polymer modifications. *Advanced Industrial and Engineering Polymer Research*, 3(2), 47-59. doi:10.1016/j.aiepr.2020.02.002
47. Qiao J., Wei G., Zhang Xiaohong, Zhang Shijun, Gao Jianming, Zhang Wei, . . . , Y. H. (2002). US 6,423,760 B1. United States Patent.
48. Rezaei Abadchi, M., & Jalali-Arani, A. (2014). The use of gamma irradiation in preparation of polybutadiene rubber nanopowder; Its effect on particle size, morphology and crosslink structure of the powder. *Nuclear Instruments and Methods in Physics Research Section B: Beam Interactions with Materials and Atoms*, 320, 1-5. doi:10.1016/j.nimb.2013.11.016
49. Rimdusit, N., Jubsilp, C., Mora, P., Hemvichian, K., Thuy, T. T., Karagiannidis, P., & Rimdusit, S. (2021). Radiation Graft-Copolymerization of Ultrafine Fully Vulcanized Powdered Natural Rubber: Effects of Styrene and Acrylonitrile Contents on Thermal Stability. *Polymers (Basel)*, 13(19). doi:10.3390/polym13193447
50. Safeeda Nv, F., Gopinathan, J., Indumathi, B., Thomas, S., & Bhattacharyya, A. (2016). Morphology and hydroscopic properties of acrylic/thermoplastic polyurethane core-shell electrospun micro/nano fibrous mats with tunable porosity. *RSC Advances*, 6(59), 54286-54292. doi:10.1039/C6RA08650K
51. Schneider, M., Pith, T., & Lambla, M. (1996). Preparation and morphological characterization of two- and three-component natural rubber-based latex particles. *Journal of Applied Polymer Science*, 62(2), 273-290. doi:https://doi.org/10.1002/(SICI)1097-4628(19961010)62:2<273::AID-APP3>3.0.CO;2-U
52. Seleem, S., Hopkins, M., Olivio, J., & Schiraldi, D. A. (2017). Comparison of Thermal Decomposition of Polystyrene Products vs. Bio-Based Polymer Aerogels. *The Ohio Journal of Science*, 117(2). doi:10.18061/ojs.v117i2.5828
53. Staverman, A. J. (1979). Science and technology of rubber, F. R. Eirich, Ed., Academic, New York, 1978, 670 pp. . *Journal of Polymer Science: Polymer Letters Edition*, 17(2). doi:https://doi.org/10.1002/pol.1979.130170209

54. Taewattana, R., Jubsilp, C., Suwanmala, P., & Rimdusit, S. (2018). Effect of gamma irradiation on properties of ultrafine rubbers as toughening filler in polybenzoxazine. *Radiation Physics and Chemistry*, *145*, 184-192. doi:10.1016/j.radphyschem.2018.02.002
55. Tian, M., Tang, Y.-W., Lu, Y.-L., Qiao, J., Li, T., & Zhang, L.-Q. (2006). Novel Rubber Blends Made from Ultra-Fine Full-Vulcanized Powdered Rubber (UFPR). *Polymer Journal*, *38*(1), 50-56. doi:10.1295/polymj.38.50
56. Tuti, I. S., Asep, H. S., Setijo, B., Dadi, R. M., & Adi, C. (2015). The effect of styrene monomer in the graft copolymerization of acrylonitrile onto deproteinized natural rubber. *International Journal of Technology*, *6*(7). doi:10.14716/ijtech.v6i7.1266
57. Wang, J., Zhang, X., Jiang, L., & Qiao, J. (2019). Advances in toughened polymer materials by structured rubber particles. *Progress in Polymer Science*, *98*, 101-160. doi:10.1016/j.progpolymsci.2019.101160
58. Wang, Q., Zhang, X., Liu, S., Gui, H., Lai, J., Liu, Y., . . . Qiao, J. (2005). Ultrafine full-vulcanized powdered rubbers/PVC compounds with higher toughness and higher heat resistance. *Polymer*, *46*(24), 10614-10617. doi:https://doi.org/10.1016/j.polymer.2005.08.074
59. Witt, E. (1959). The effect of polymer composition on radiation-induced crosslinking. *Journal of Polymer Science*, *41*(138), 507-518. doi:https://doi.org/10.1002/pol.1959.1204113844
60. Wongkumchai, R., Amornkitbamrung, L., Mora, P., Jubsilp, C., & Rimdusit, S. (2021). Effects of coagent incorporation on properties of ultrafine fully vulcanized powdered natural rubber prepared as toughening filler in polybenzoxazine. *SPE Polymers*, *2*(3), 191-198. doi:https://doi.org/10.1002/pls2.10038
61. Wongthong, P., Nakason, C., Pan, Q., Rempel, G. L., & Kiatkamjornwong, S. (2013). Modification of deproteinized natural rubber via grafting polymerization with maleic anhydride. *European Polymer Journal*, *49*(12), 4035-4046. doi:10.1016/j.eurpolymj.2013.09.009
62. Wu, F., Xie, T., & Yang, G. (2010). Properties of toughened poly(butylene terephthalate) by blending with reactive ultra-fine full-vulcanized acrylonitrile butadiene rubber particles (UFNBRP). *Polymer Bulletin*, *65*(7), 731-742. doi:10.1007/s00289-010-0281-2
63. Xue, T. J., McKinney, M. A., & Wilkie, C. A. (1997). The thermal degradation of polyacrylonitrile. *Polymer degradation and stability*, *58*, 193-202.
64. Yu, S., Hu, H., Ma, J., & Yin, J. (2008). Tribological properties of epoxy/rubber nanocomposites. *Tribology International*, *41*(12), 1205-1211. doi:10.1016/j.triboint.2008.03.001

Figures

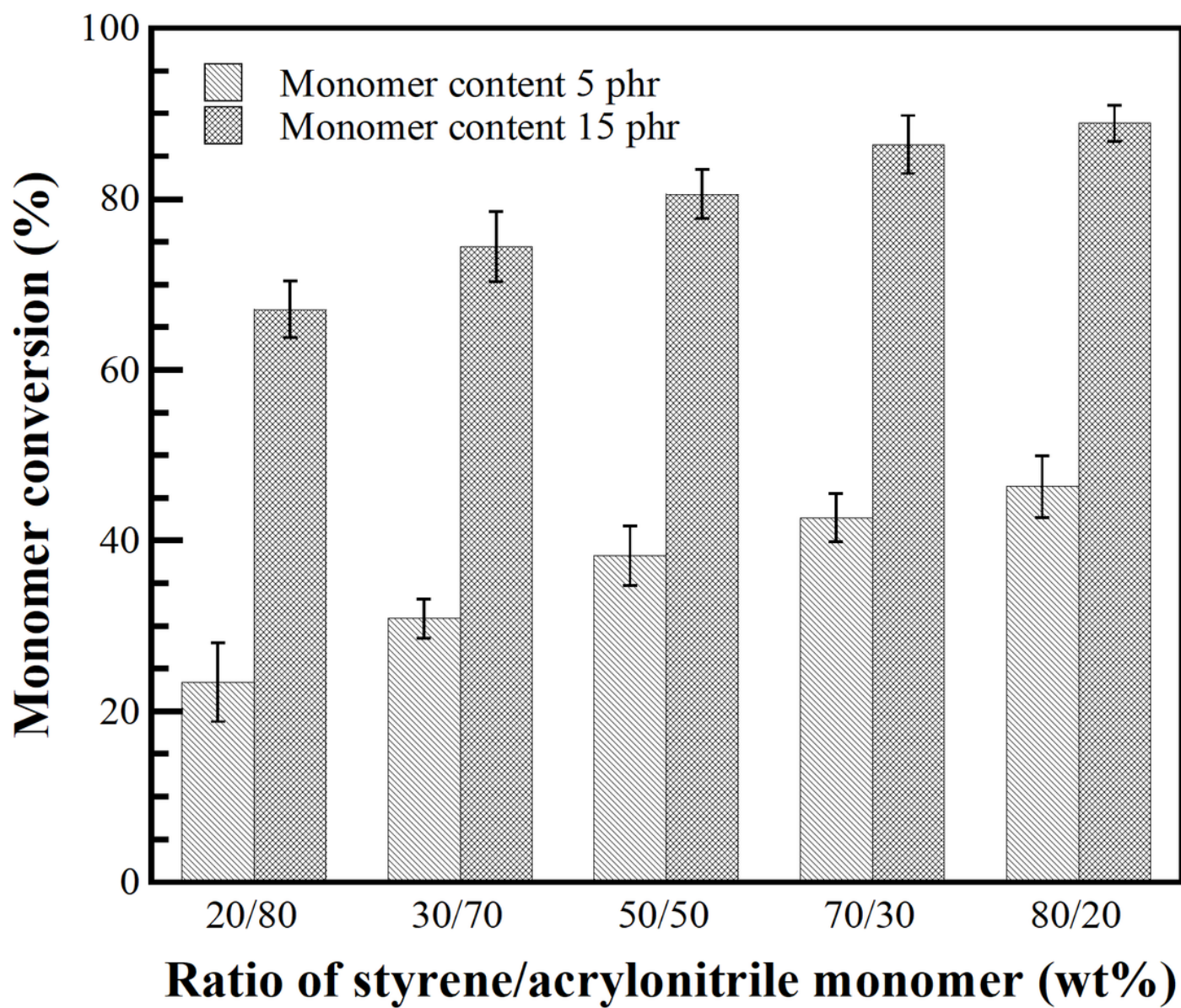


Figure 1

Variation of St/AN weight ratio as a function of monomer conversion (%) at different monomer content.

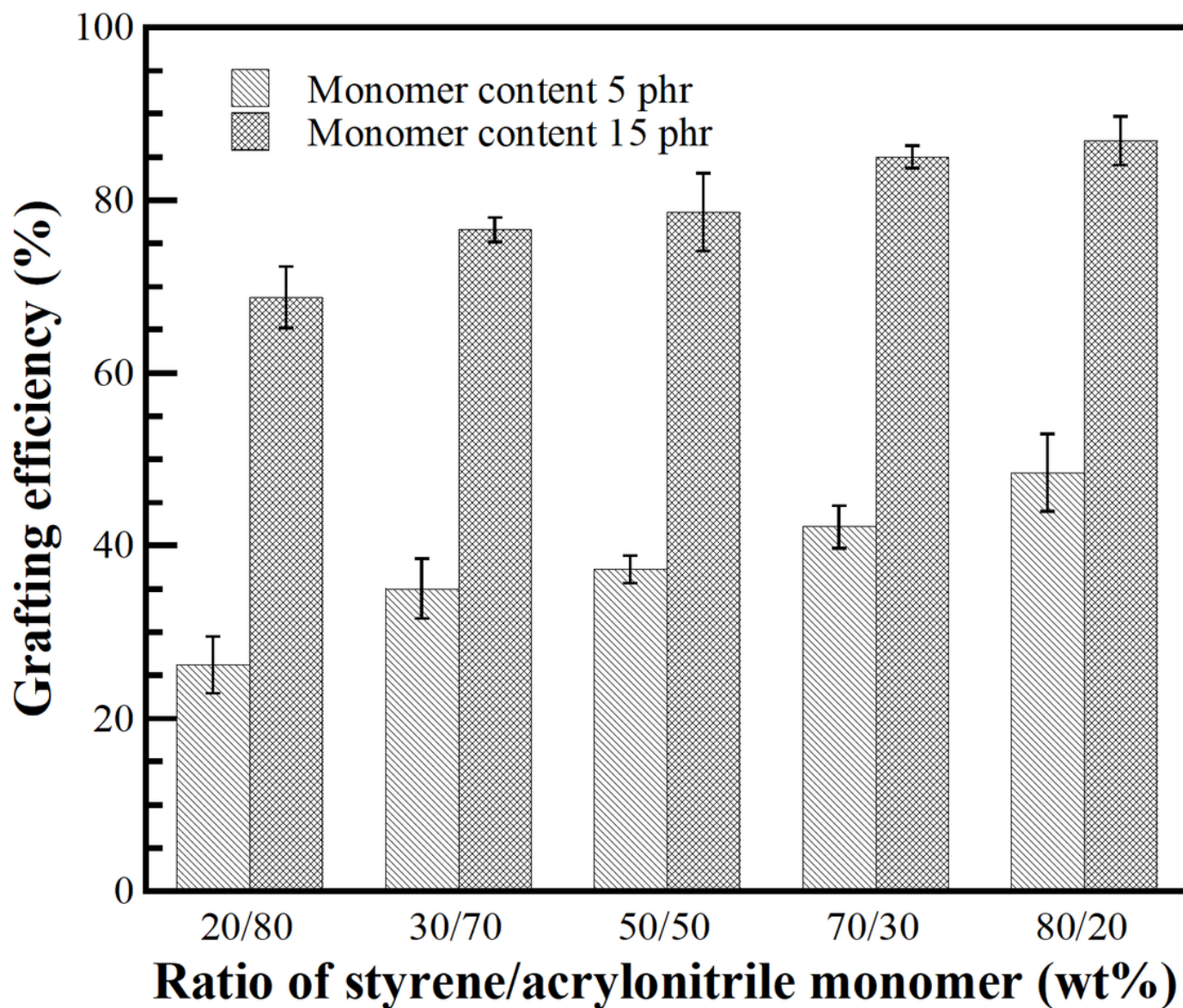


Figure 2

Variation of St/AN weight ratio as a function of grafting efficiency (%) at different monomer content.

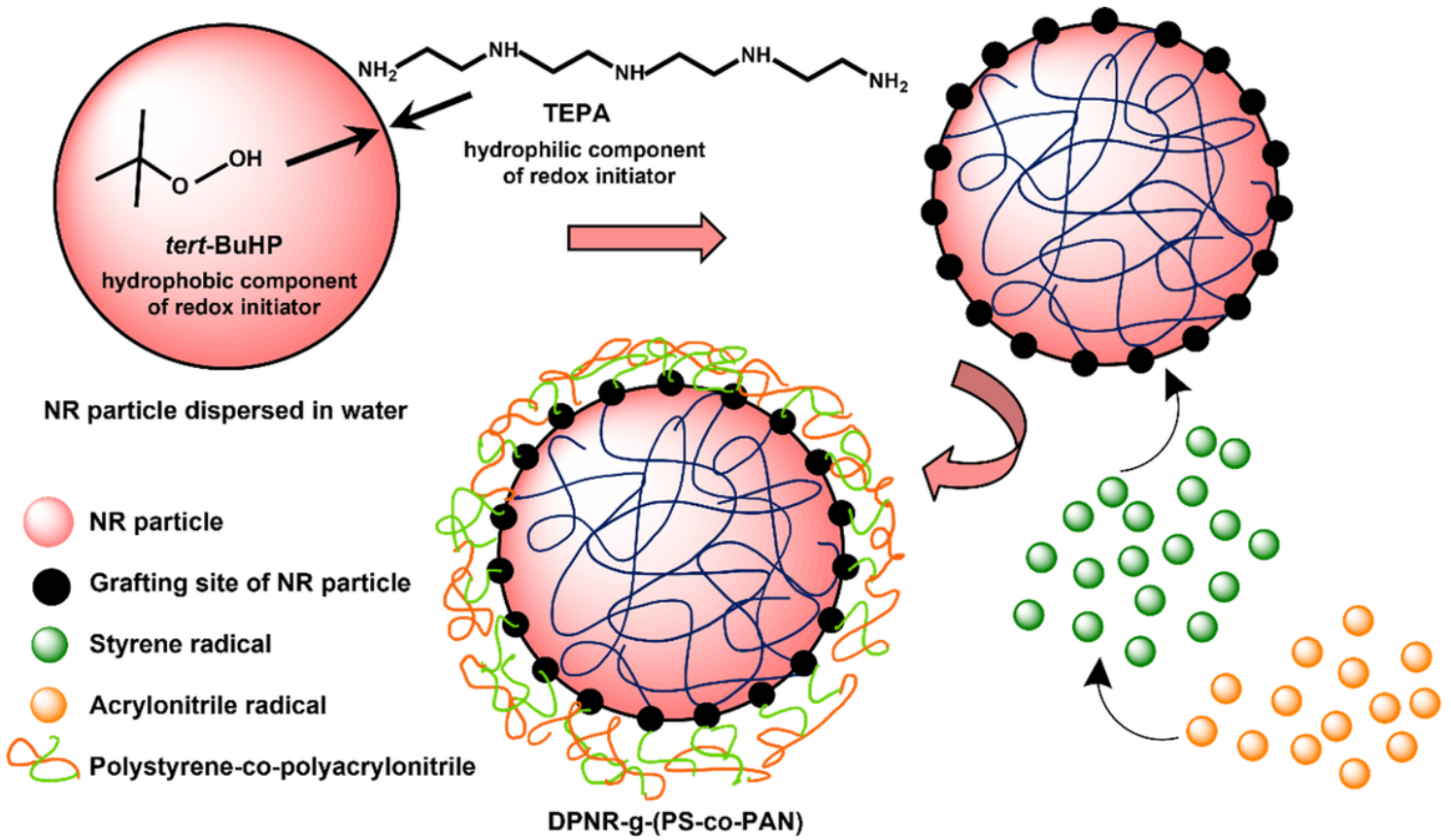


Figure 3

Possible reaction sites in the modified NR latex in the bipolar redox initiation systems (adapted from (Schneider et al., 1996)).

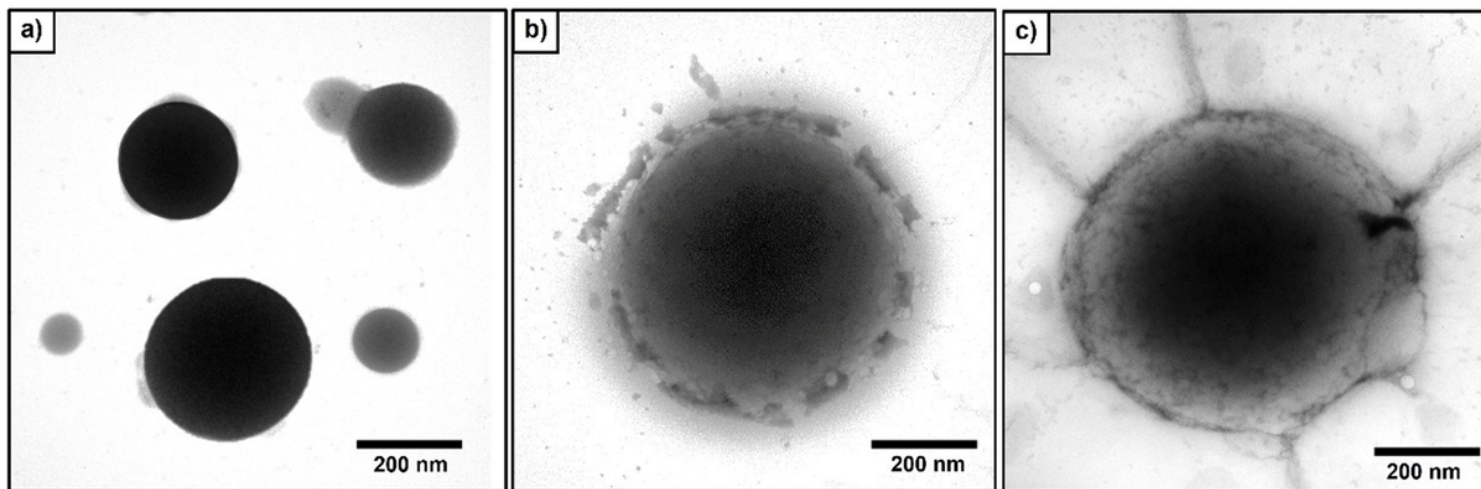


Figure 5

TEM micrographs of a) Virgin NR b) DPNR-g-(PS-co-PAN) at monomer content: 5 phr and c) DPNR-g-(PS-co-PAN) at monomer content 15 phr (100,000×magnification).

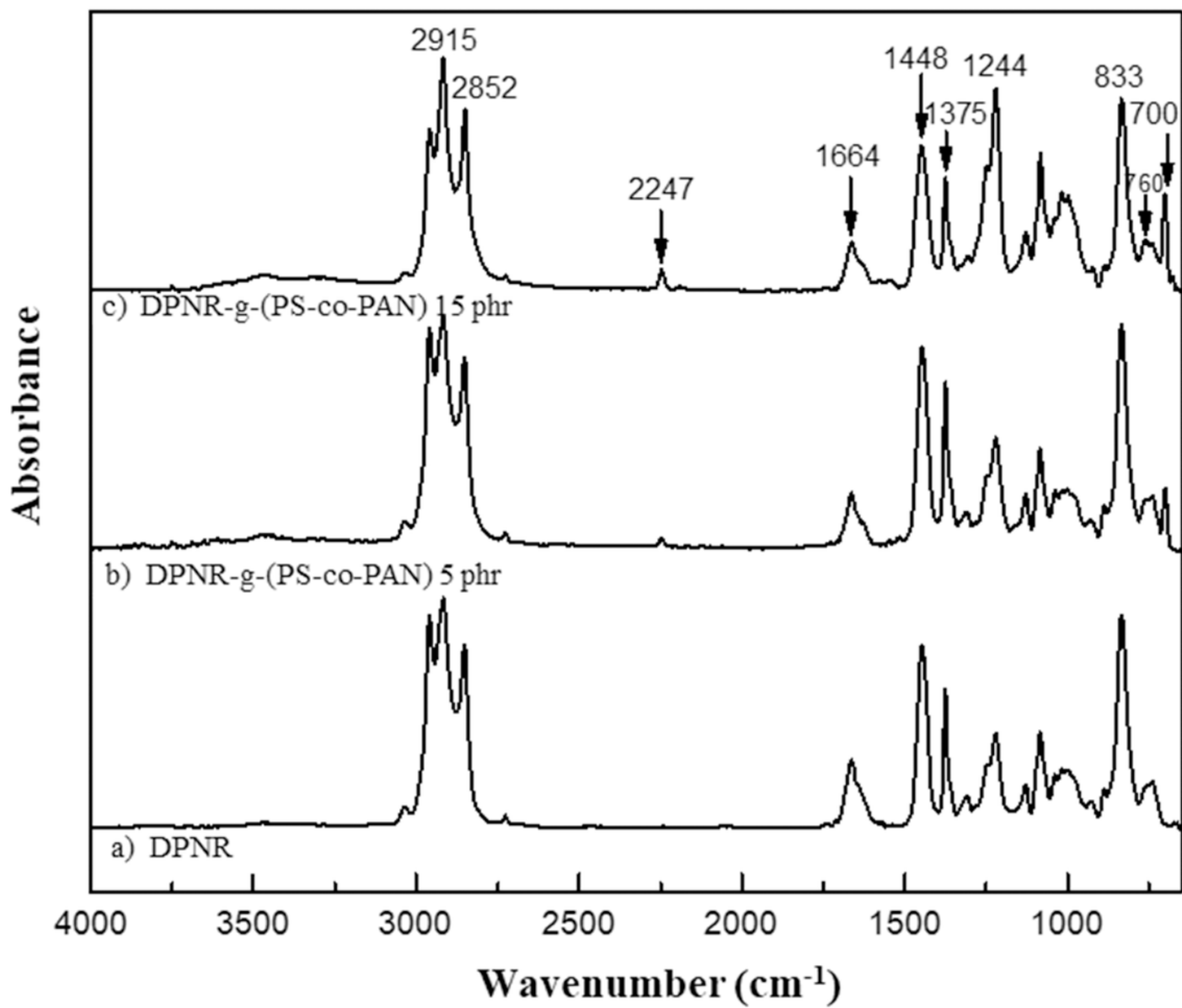


Figure 6

FTIR spectra DPNR and DPNR-g-(PS-co-PAN) at different monomer content.

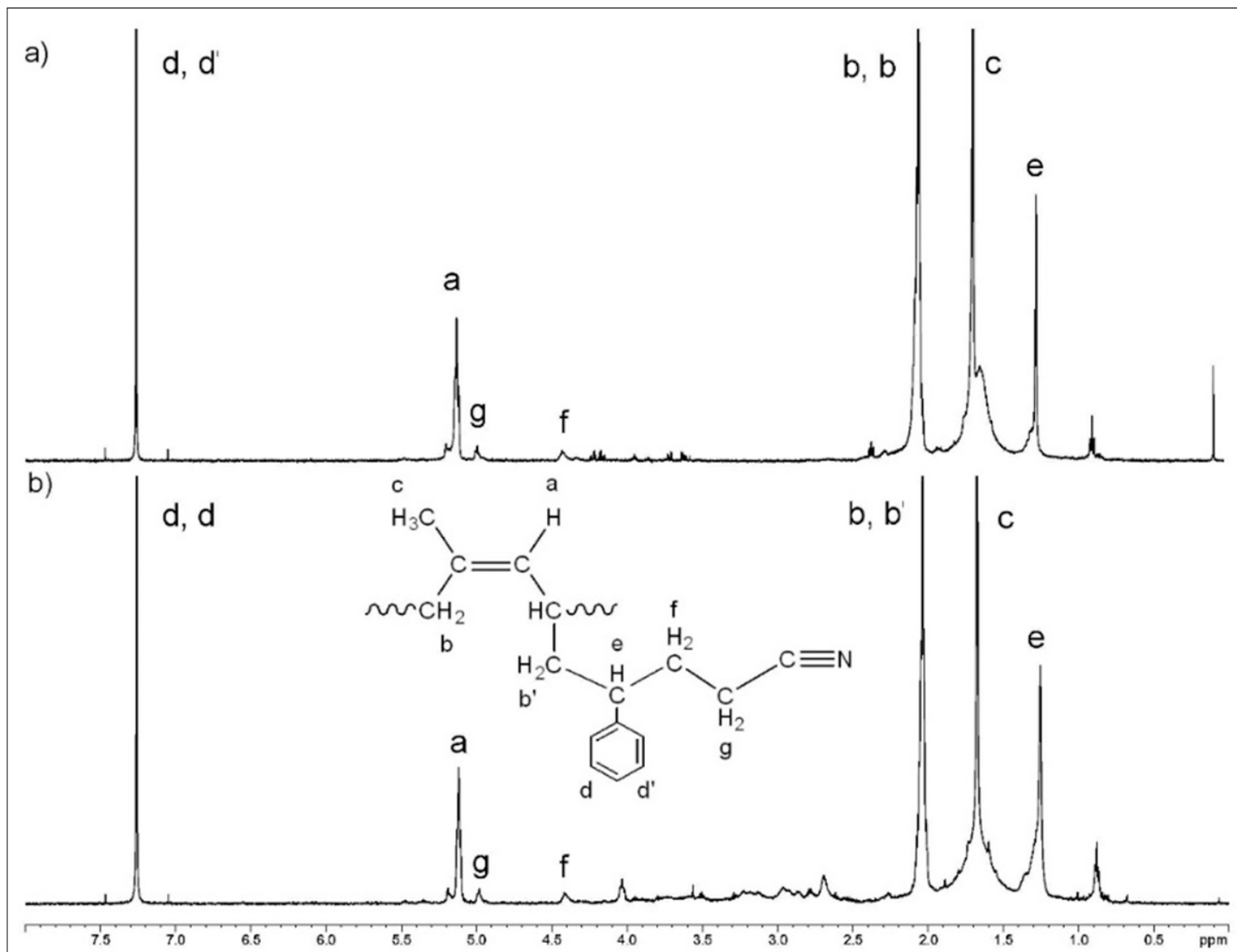


Figure 7

$^1\text{H-NMR}$ spectra of DPNR-g-(PS-co-PAN) at different monomer content.

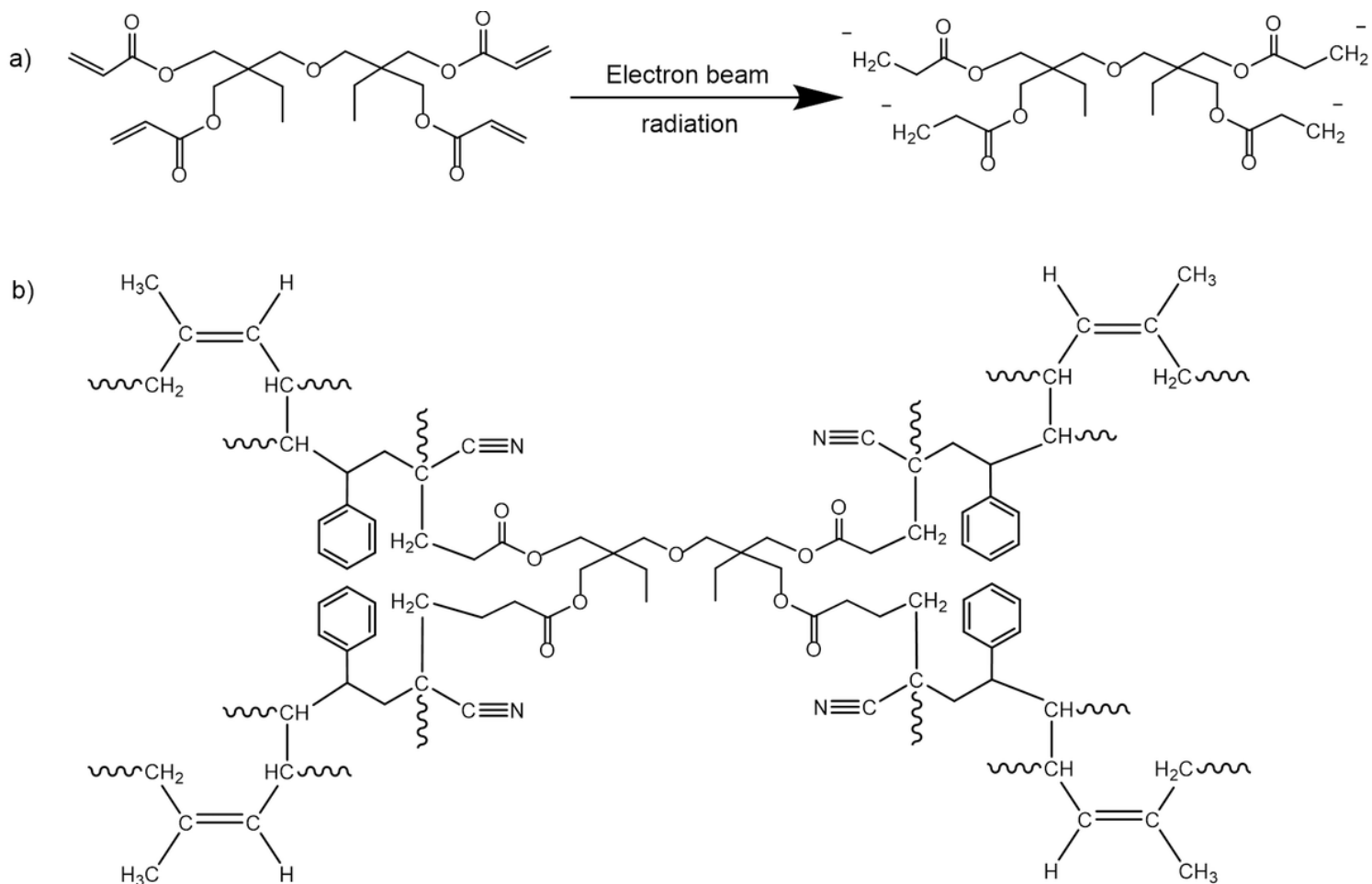


Figure 8

a) DTMPTA structure was radiated by electron beam b) possible structure of crosslinked UFPNR-g-(PS-co-PAN) in the presence of DTMPTA.

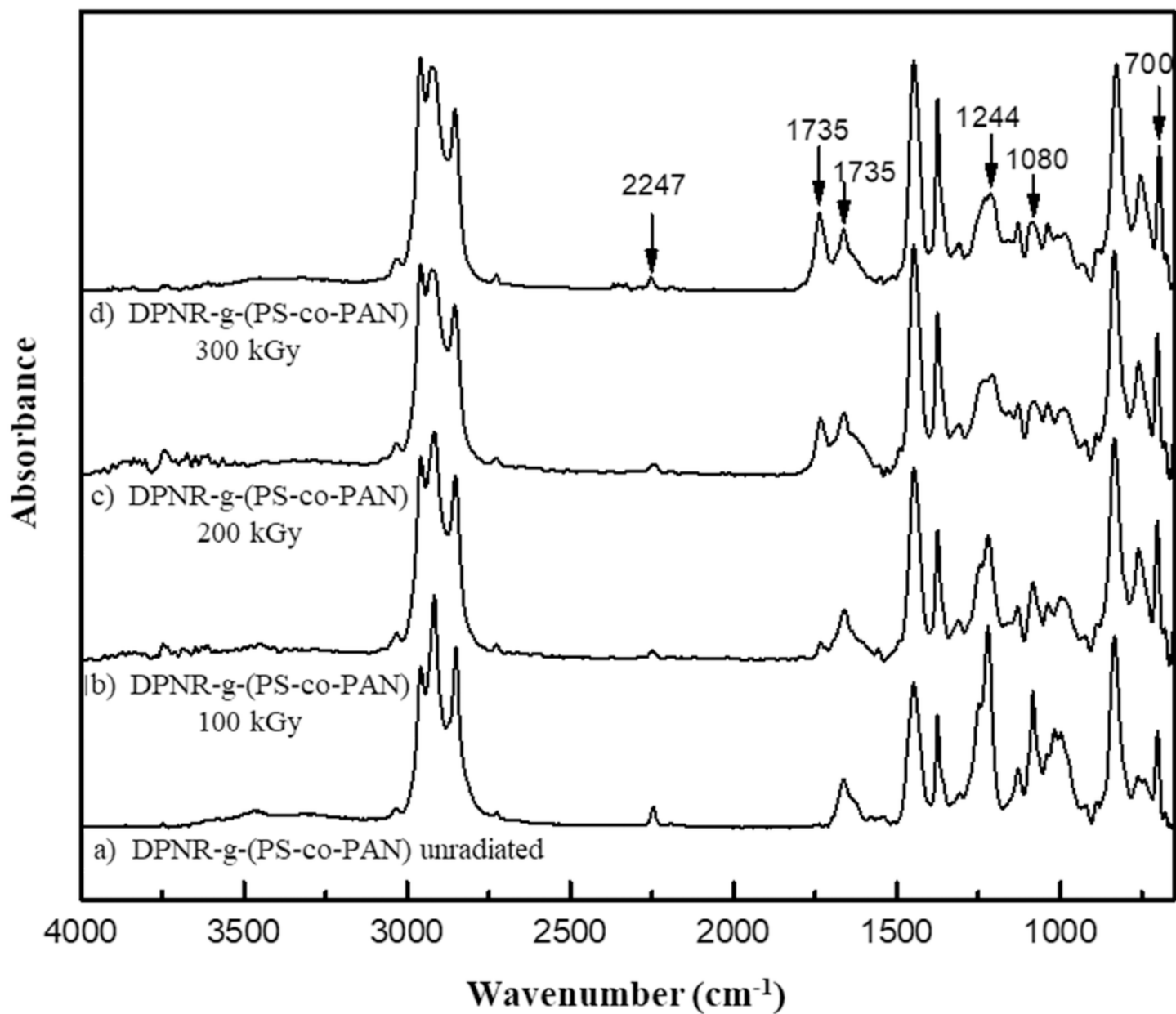


Figure 9

FTIR spectra of grafted NR at monomer content 15 phr with St/AN weight ratio 80/20 at various irradiation doses: a) unirradiated, b) 100, c) 200, and d) 300 kGy.

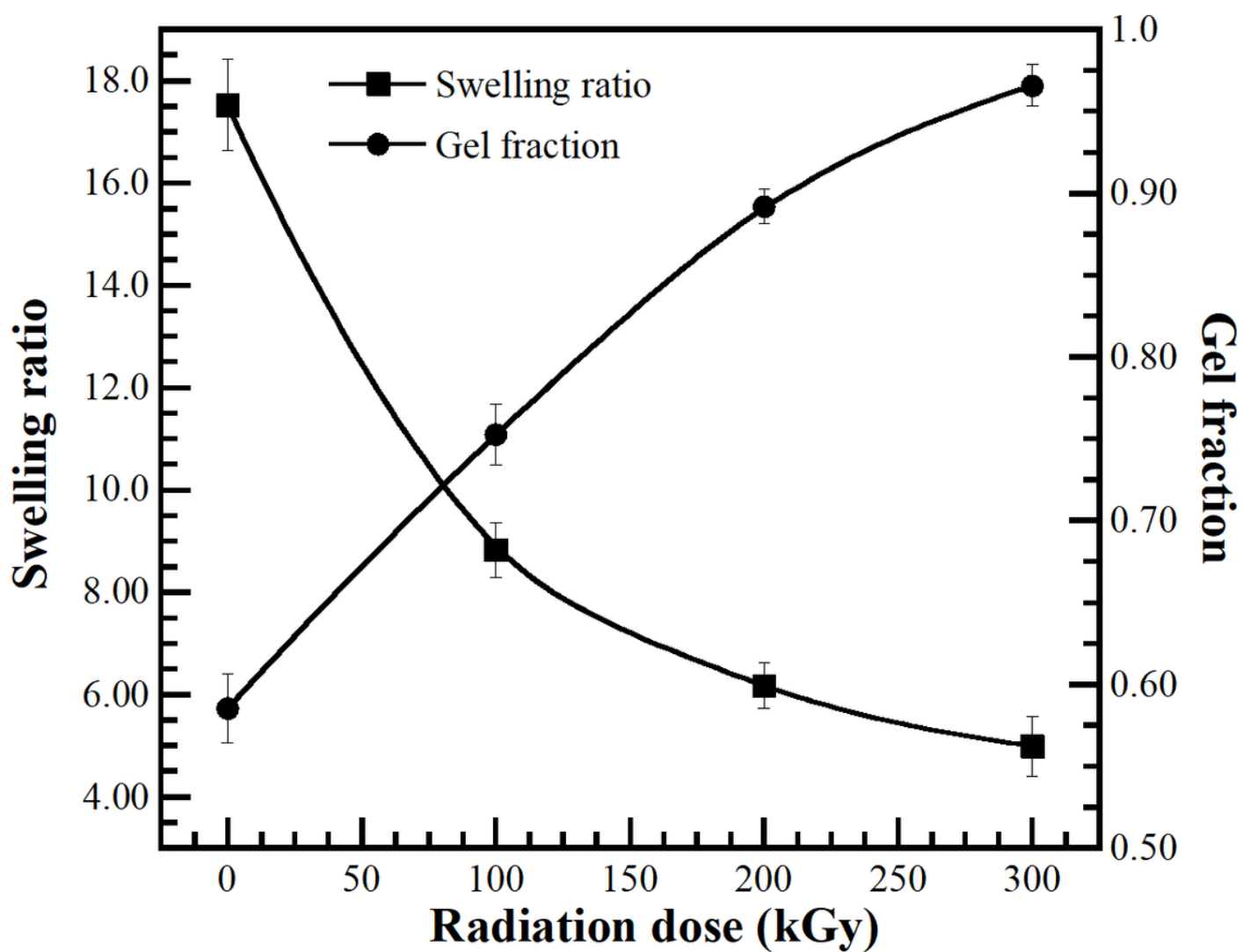


Figure 10

(■) Swelling ratio and (•) gel fraction of UFPNR-g-(PS-co-PAN) 15 phr with ST/AN weight ratio 80/20 at various irradiation doses.

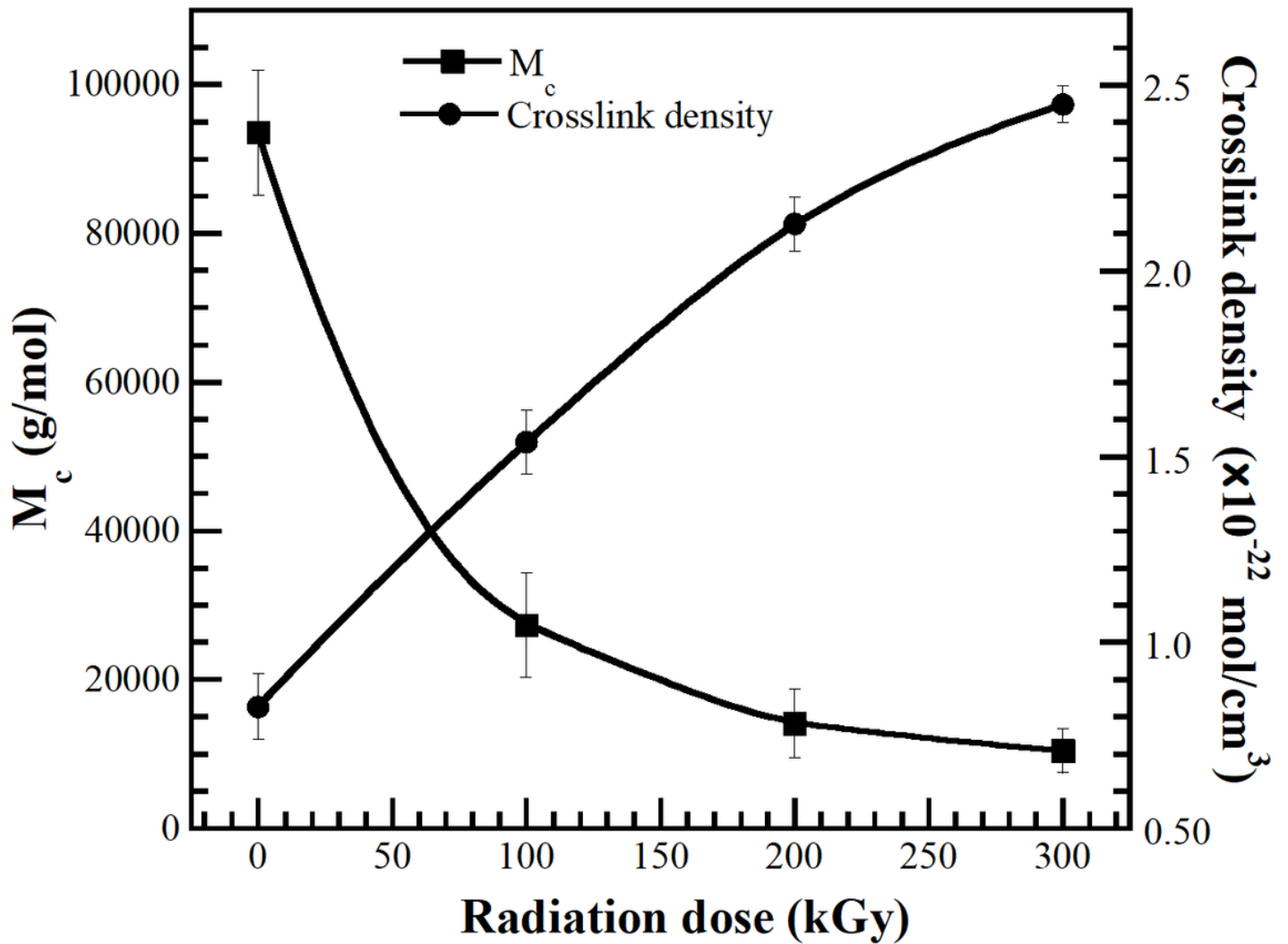


Figure 11

(■) Molecular weight between crosslinks (M_c) and (•) crosslink density of UFPNR-g-(PS-co-PAN) 15 phr with St/AN weight ratio 80/20 at various irradiation doses.

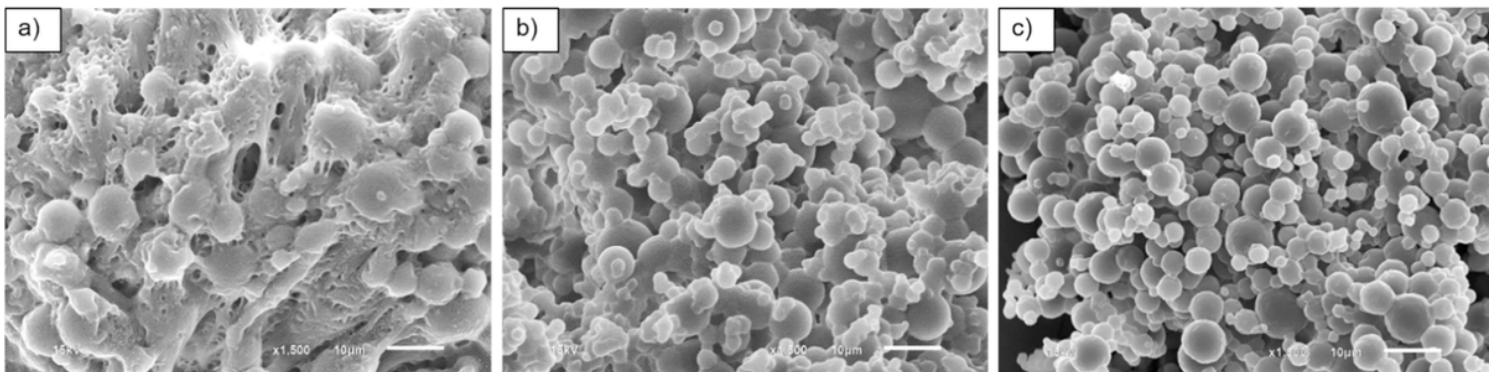


Figure 12

SEM micrographs ($\times 1500$ magnification) of UFPNR-g-(PS-co-PAN) at monomer content 5 phr with various irradiation doses: a) 100 kGy, b) 200 kGy, d) 300 kGy.

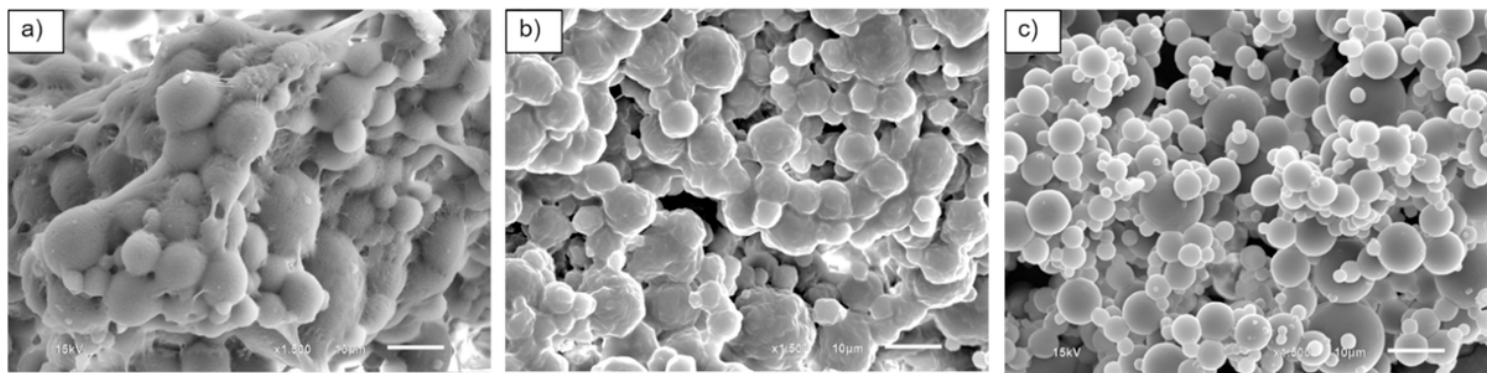


Figure 13

SEM micrographs ($\times 1500$ magnification) of UFPNR-g-(PS-co-PAN) at monomer content 15 phr with various irradiation doses: a) 100 kGy, b) 200 kGy, d) 300 kGy.

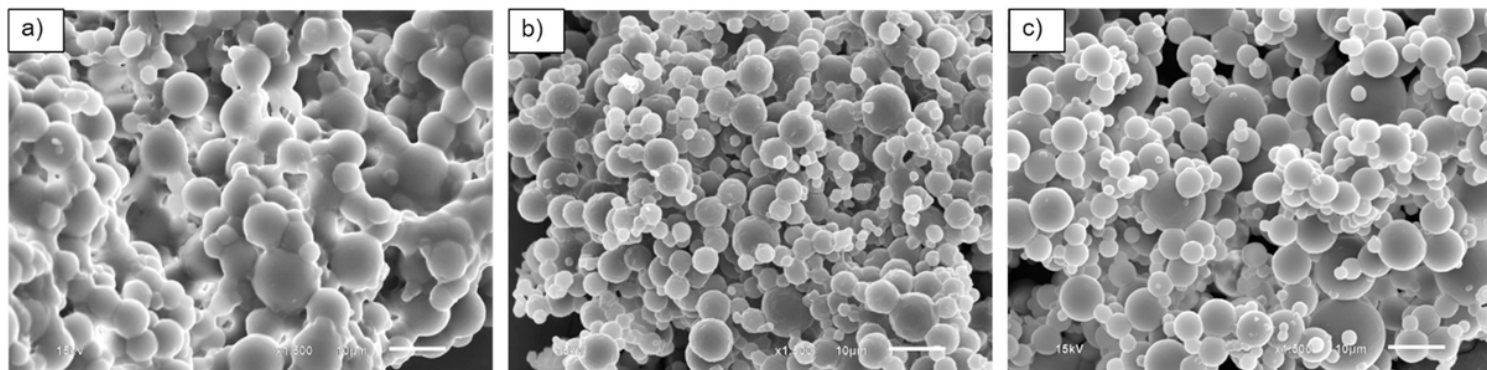


Figure 14

SEM micrographs ($\times 1500$ magnification) of a) virgin UFPNR and UFPNR-g-(PS-co-PAN) at monomer content b) 5 and c) 15 phr at irradiation dose 300 kGy.

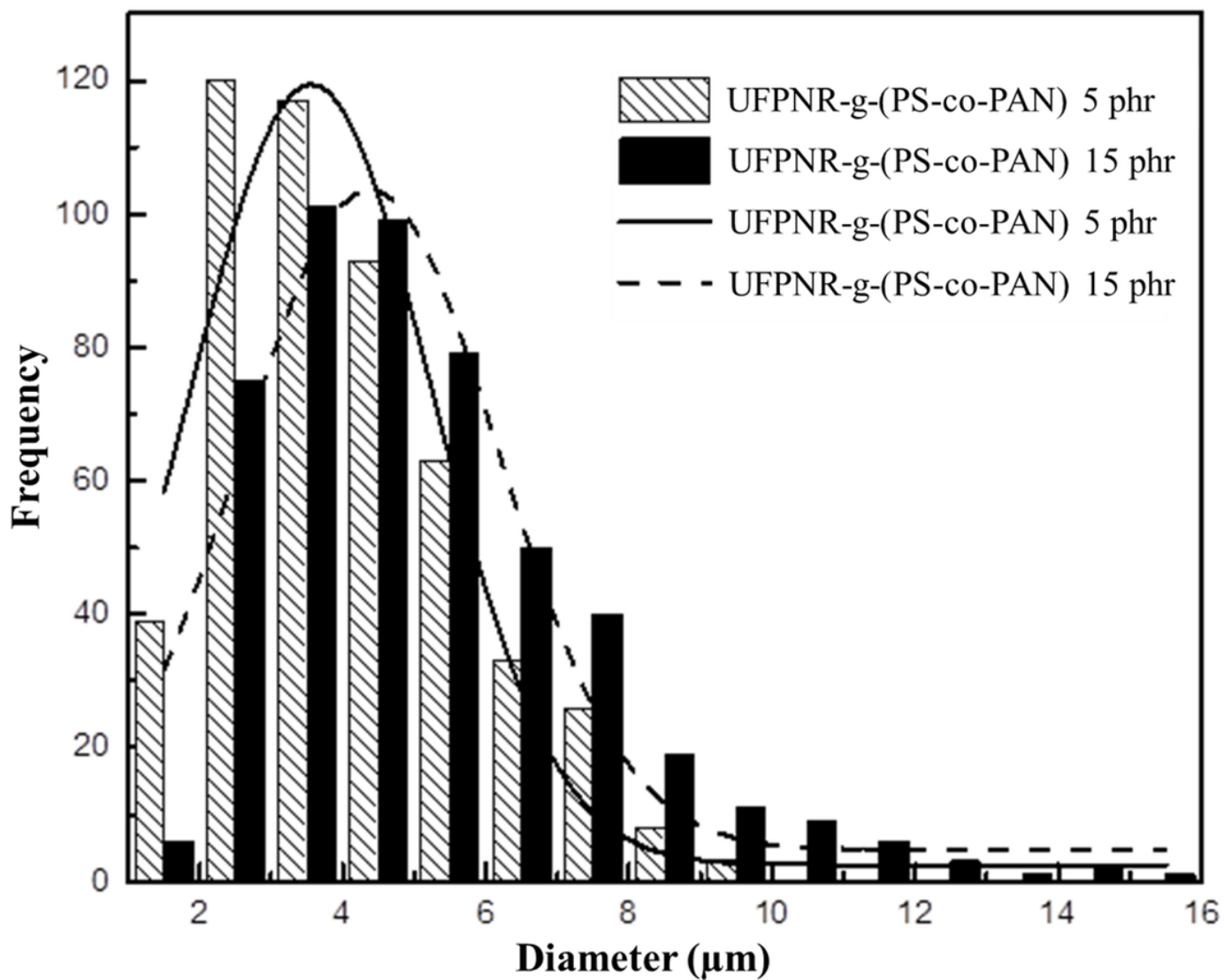


Fig. 15 Particle sizes of the modified UFPNR with monomer content (▨) 5 and (■) 15 phr at irradiation doses 300 kGy.

Figure 15

See image above for figure legend

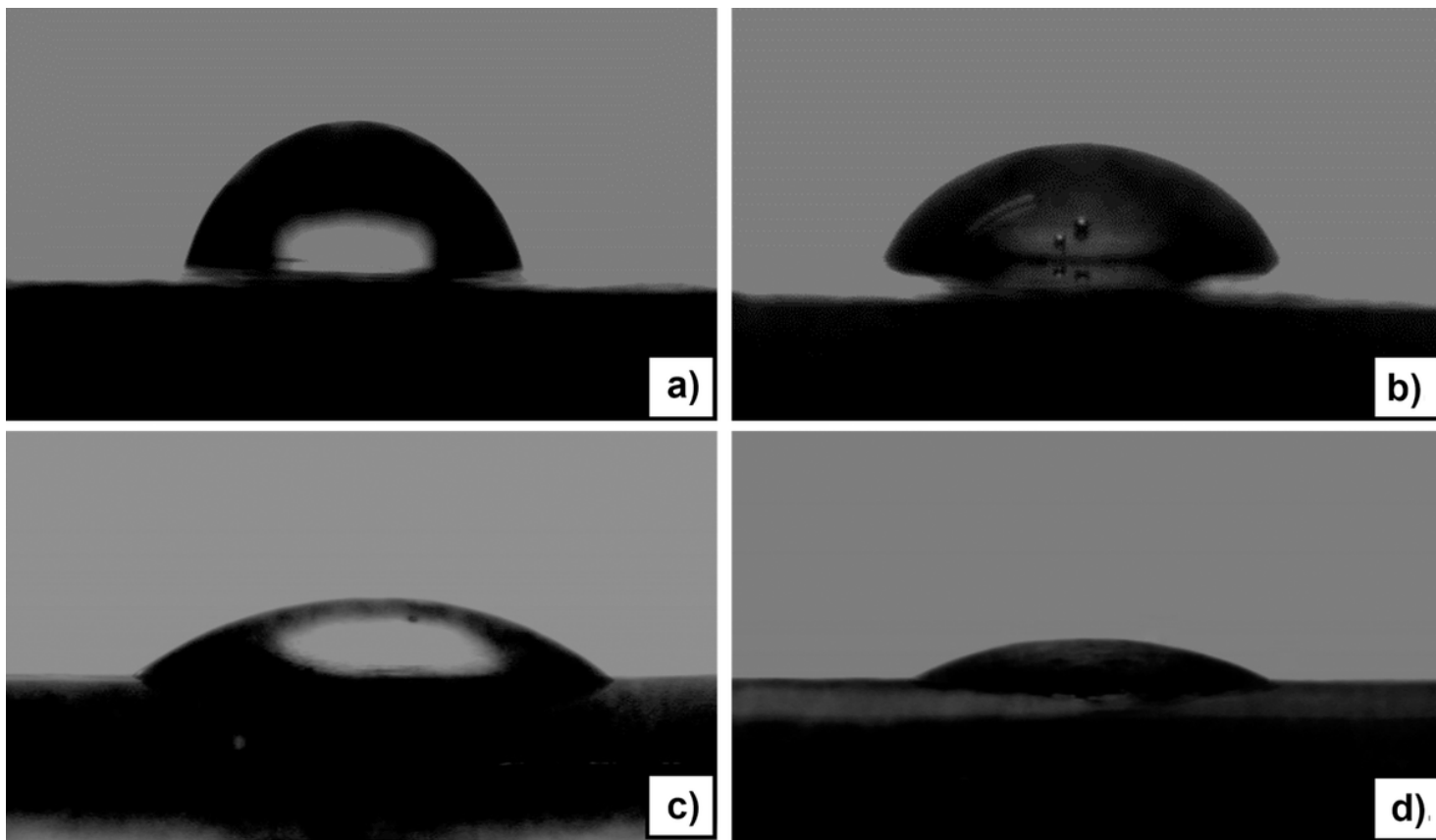


Figure 16

Contact angles of a water droplet on surfaces of NR films after irradiation a) unmodified NR and grafted NR at monomer content 15 phr with various St/AN monomer weight ratios containing; b) 80/20, c) 50/50, and d) 20/80 wt%.

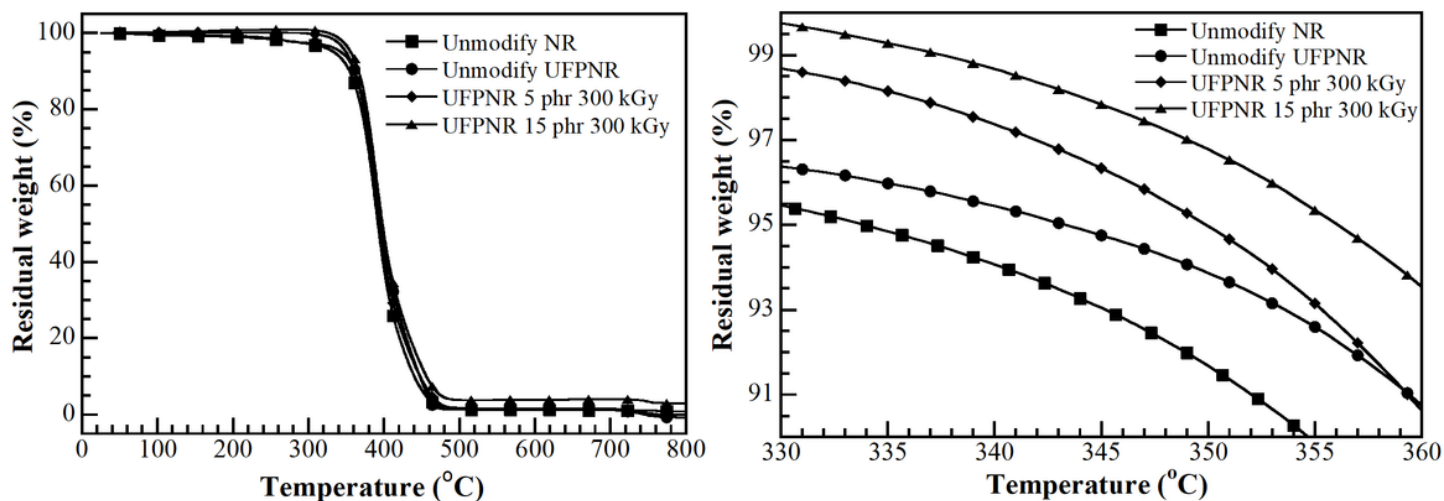


Fig. 17 The degradation temperature at 5% weight loss (T_{d5}) (■) unmodified NR, (●) unmodified UFPNR at irradiation dose 300 kGy, and UFPNR-g-(PS-co-PAN) at monomer content (◆) 5 phr and (▲) 15 phr at irradiation dose 300 kGy

Figure 17

See image above for figure legend

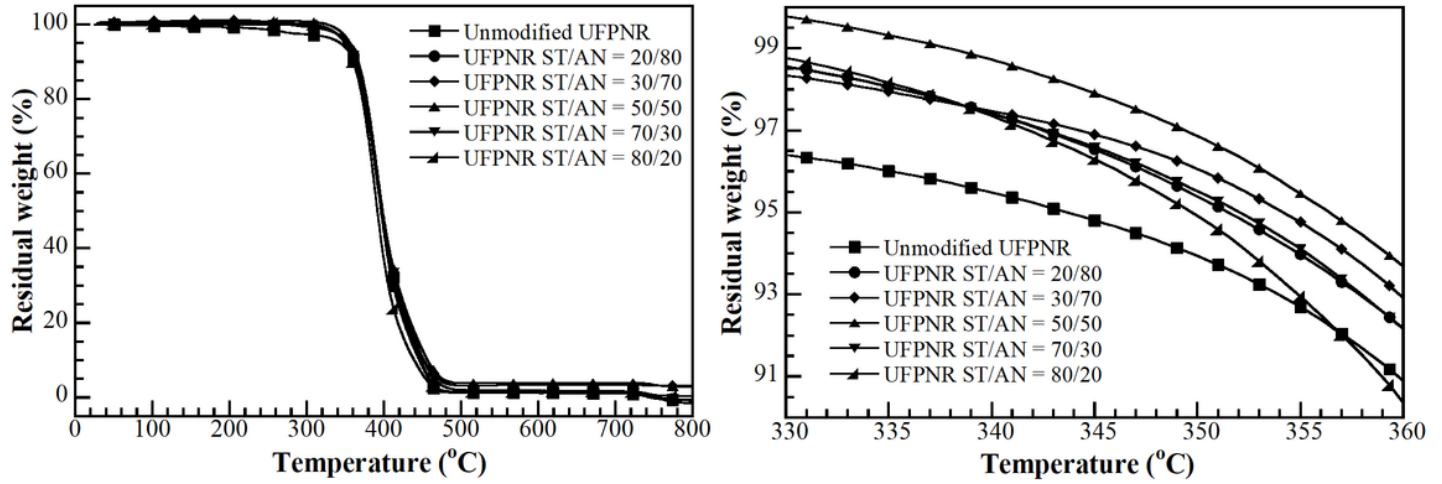


Fig. 18 The degradation temperature at 5 % weight loss (T_{d5}) (■) unmodified UFPNR at irradiation dose 300 kGy and UFPNR-g-(PS-co-PAN) at monomer content 15 phr with St/AN weight ratios: (●) 20/80, (◆) 30/70, (▲) 50/50, (▼) 70/30 and (▲) 80/20 at irradiation dose 300 kGy

Figure 18

See image above for figure legend

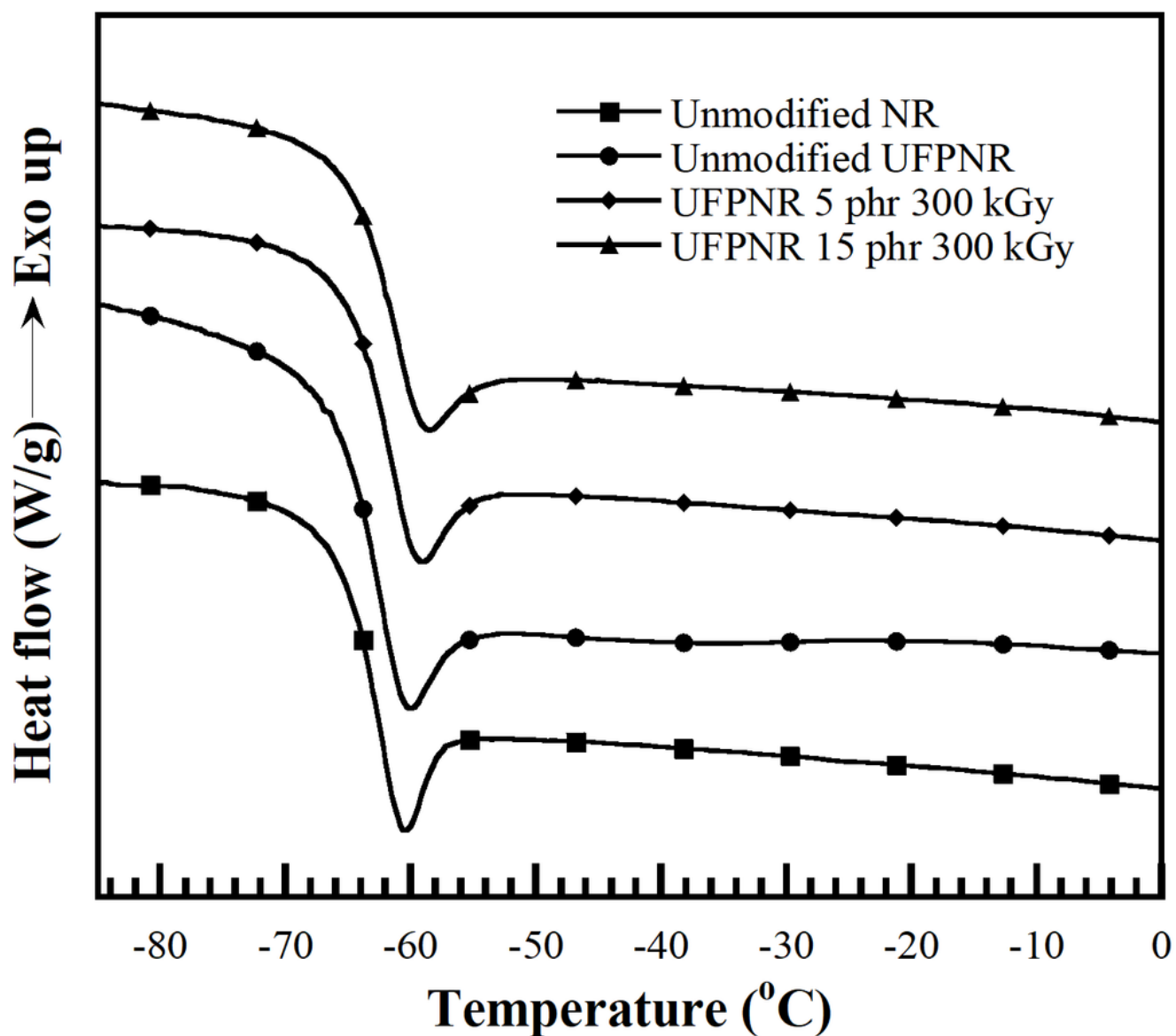


Figure 19 Glass transition temperature of (■) unmodified NR, (●) unmodified UFPNR at irradiation dose 300 kGy, and UFPNR-g-(PS-co-PAN) at monomer content (◆) 5 phr and (▲) 15 phr at irradiation dose 300 kGy

Figure 19

See image above for figure legend

Supplementary Files

This is a list of supplementary files associated with this preprint. Click to download.

- [GraphicalAbstract.tif](#)